

**Self-Assembly and Anion sensing of Metal-organic [M₆L₂]
Cages from Fluorescent Triphenylamine Tri-pyrazoles with
Dipalladium(II,II) Corners**

Table of Contents

1. NMR and MS data

¹H NMR and ¹³C NMR of all the compounds

2D COSY NMR

ESI-MS

2. X-ray diffraction measurement

Crystal structures data

ORTEP diagram of the molecular structures

3. Research for fluorescence properties

4. References

Supporting Information

Materials

All chemicals and solvents were reagent grade and were purified according to conventional methods.¹ The metal complexes $[(\text{bpy})_2\text{Pd}_2(\text{NO}_3)_2](\text{NO}_3)_2$, $[(\text{dmbpy})_2\text{Pd}_2(\text{NO}_3)_2](\text{NO}_3)_2$ and $[(\text{phen})_2\text{Pd}_2(\text{NO}_3)_2](\text{NO}_3)_2$ were prepared according to literature procedures.²

Instrumentation

^1H NMR, ^{13}C NMR and 2D COSY NMR experiments were performed at 400 MHz on a Bruker Avance III HD 400 spectrometer using tetramethylsilane. ESI-MS measurements were performed with a JEOL Accu-TOF mass spectrometer.

X-Ray structural determinations

X-Ray diffraction data of the crystals of complex **1**·6PF₆⁻ were carried out at 291 K using synchrotron radiation ($\lambda = 0.80010 \text{ \AA}$) via the 3W1A in the IHEP with the approval of the Beijing Synchrotron Radiation Facility (BSRF). The diffraction data reduction and integration were performed by the HKL2000 software. Most of the non-hydrogen atoms were found using the direct methods program in the Bruker SHELXTL software.

Data for **2**·6PF₆⁻ and **3**·6PF₆⁻ were collected at 123 K on a Bruker Smart Apex CCD area detector equipped with a graphite monochromated MoK α radiation ($\lambda = 0.71073 \text{ \AA}$). All the structures were solved by direct methods and refined employing full-matrix least-squares on F² by using SHELXTL (Bruker, 2000) program and expanded using Fourier techniques.³⁻⁴ All non-H atoms of the complexes were refined with anisotropic thermal parameters. The hydrogen atoms were included in idealized positions. In complexes **2**·12PF₆⁻ and **3**·12PF₆⁻, the unit cell includes a large region of disordered solvent acetonitrile molecules, which could not be modelled as discrete atomic sites. We employed PLATON/SQUEEZE to calculate the diffraction contribution of the solvent acetonitrile molecules, thereby, to produce a set of solvent-free CH₃CN. Final residuals along with the unit cell, space group, data collection and

refinement parameters are presented in Table S1.

General procedures

Cage 1 (1·6PF₆⁻) Combination of dimetal corners [(bpy)₂Pd₂(NO₃)₂](NO₃)₂ (25 mg, 0.034 mmol) with a suspension of **H₃L** (9.6 mg, 0.022 mmol) in H₂O (2 ml) and acetone(2 ml), the mixture was stirred for 24 h at room temperature, then removed to the oil-bath of 60 °C and continued stirring for 8 h via a directed self-assembly approach that involves spontaneous deprotonation of the 1H-tripyranyl ligands in aqueous solution. Based on preliminary NMR data, gave the desired product 1·6NO₃⁻, as a light-yellow precipitate. A ten-fold excess of KPF₆ was added to the solution which resulted in an immediate deposition, the mixture was continued stirring for 6 h, then the precipitation was filtered, washed with minimum amount of cold water and dried in vacuum to give high yield (87%) of **1** as yellow solid.

The NO₃⁻ salt of **1** as a light-yellow precipitate, ¹H NMR (400 MHz, D₂O, 25 °C, ppm), δ = 8.47-8.43 (d, 12H, bpy-H_{a1}, bpy-H_{b1}), 8.43-8.41 (m, 12H, bpy-H_{c1}), 8.39-8.38 (m, 12H, bpy-H_{a2}, bpy-H_{b2}), 8.34-8.32 (d, 12H, bpy-H_{c2}), 7.78-7.75, 7.66-7.64 (m, 12H, bpy-H_{d1}, bpy-H_{d2}), 8.13, 6.99 (d, 12H, Pz-H₂, H₄), 8.54-8.52, 6.93-6.91 (d, 12H, Ar-H₁, H₃). Elemental analyses calcd (%) for C₁₁₄H₈₄N₃₂O₁₈Pd₆: C, 48.41; H, 2.99; N, 15.84; Found: C, 48.10; H, 3.08; N, 15.90.

The PF₆⁻ salt of **1** was obtained as yellow needle crystal in quantitative yield. ¹H NMR (400 MHz, CD₃CN, 25 °C, ppm), δ = 8.35-8.30 (d, 12H, bpy-H_{a1}, bpy-H_{b1}), 8.27-8.26 (m, 12H, bpy-H_{c1}), 8.26-8.23 (m, 12H, bpy-H_{a2}, bpy-H_{b2}), 7.85-7.84 (m, 12H, bpy-H_{c2}), 7.69-7.63, 7.51-7.45 (m, 12H, bpy-H_{d1}, bpy-H_{d2}), 7.84, 6.82 (d, 12H, Pz-H₂, H₄), 8.37-8.35, 6.95-6.93 (d, 12H, Ar-H₁, H₃). ¹³C NMR (100 MHz, CD₃CN, 25 °C, ppm): δ 157.88, 157.01, 151.22, 151.18, 151.02, 143.62, 142.96, 142.84, 128.56, 127.81, 125.40, 124.87, 124.73, 124.62, 107.24, 68.46, 22.80. ESI-MS (CH₃CN, m/z): 1517.81, 963.54 for [1·4PF₆⁻]²⁺, [1·3PF₆⁻]³⁺. Elemental analyses calcd (%) for C₁₁₄H₈₄N₂₆F₃₆P₆Pd₆: C, 41.10; H, 2.53; N, 10.9; Found: C, 41.2; H, 2.62; N, 10.66.

Cage 2 (2·6PF₆⁻) [(dmbpy)₂Pd₂(NO₃)₂](NO₃)₂ (25 mg, 0.030 mmol) was treated with **H₃L** (8.9 mg, 0.020 mmol) at a ratio of 3:2 in H₂O (3 ml) and acetone (2 ml), the

mixture was stirred for 24 h at room temperature then removed to the oil-bath of 60 °C and continued stirring for 8 h. A ten-fold excess of KPF₆ was added to the solution which resulted in an immediate deposition, the mixture was continued stirring for 6 h, then the precipitation was filtered, washed with minimum amount of cold water and dried in vacuum to give high yield (83%) of **2·6PF₆⁻** as yellow solid.

The NO₃⁻ salt of **2** as a light-yellow precipitate, ¹H NMR (400 MHz, D₂O, 25 °C, ppm) δ = 7.80, 7.72 (d, 12H, dmbpy-H_{a1}, dmbpy-H_{a2}), 7.80-7.78, 7.44-7.43 (d, 12H, dmbpy-H_{b1}, dmbpy-H_{b2}), 7.13-7.12, 6.99-6.97 (m, 12H, dmbpy-H_{c1}, dmbpy-H_{c2}), 2.18, 2.09 (s, 36H, dmbpy-H_{d1}, dmbpy-H_{d2}), 7.55, 6.49 (d, 12H, Pz-H₂, H₄), 8.03-8.01, 6.47-6.45(d, 12H, Ar-H₁, H₃). Elemental analyses calcd (%) for C₁₂₆H₁₂₀N₃₂O₁₈Pd₆: C, 50.29; H, 4.02; N, 14.89; Found: C, 50.38; H, 4.12; N, 14.92.

The PF₆⁻ salt of **2** was obtained as red needle-shaped crystal in quantitative yield. ¹H NMR (400 MHz, CD₃CN, 25 °C, ppm) δ = 8.21, 8.08 (d, 12H, dmbpy-H_{a1}, dmbpy-H_{a2}), 8.08-8.06, 7.65-7.63 (d, 12H, dmbpy-H_{b1}, dmbpy-H_{b2}), 7.48-7.46, 7.28-7.27 (m, 12H, dmbpy-H_{c1}, dmbpy-H_{c2}), 2.58, 2.51 (s, 36H, dmbpy-H_{d1}, dmbpy-H_{d2}), 7.81-7.80, 6.79-6.78 (d, 12H, Pz-H₂, H₄), 8.33-8.31, 6.94-6.92 (d, 12H, Ar-H₁, H₃). ¹³C NMR (100 MHz, CD₃CN, 25°C, ppm): δ 157.32, 156.54, 155.94, 151.08, 150.18, 147.83, 143.58, 128.88, 127.82, 125.61, 125.25, 124.88, 107.12, 68.45, 22.80, 21.80, 21.28, 21.26. ESI-MS (CH₃CN, m/z): 728.73, 1019.63, 1603.42 for [2·2PF₆⁻]⁴⁺, [2·3PF₆⁻]³⁺, [2·4PF₆⁻]²⁺. Elemental analyses calcd (%) for C₁₂₆H₁₂₀N₂₆F₃₆P₆Pd₆ : C, 43.30; H, 3.47; N, 10.42; Found: C, 41.21; H, 4.32; N, 10.45.

Cage 3 (3·6PF₆⁻) [(phen)₂Pd₂(NO₃)₂](NO₃)₂ (25 mg, 0.029 mmol) was treated with **H₃L** (8.5 mg, 0.019 mmol) at a ratio of 3:2 in H₂O (3 ml) and acetone (2 ml) and the mixture was stirred for 24 h at room temperature then removed to the oil-bath of 60 °C and continued stirring for 8 h. A ten-fold excess of KPF₆ was added to the solution which resulted in an immediate deposition, the mixture was continued stirring for 6 h, then the precipitation was filtered, washed with minimum amount of cold water and dried in vacuum to give high yield (78%) of **3·6PF₆⁻** as yellow solid.

The NO₃⁻ salt of **3** as a light-yellow precipitate, ¹H NMR (400 MHz, D₂O , 25 °C): δ = 8.77-8.75, 8.72-8.70 (m, 12H, phen-H_{a1}, phen-H_{a2}), 8.68-8.66, 8.31-8.30 (m, 12H, phen-H_{b1}, phen-H_{b2}), 8.06, 7.95 (s, 12H, phen-H_{c1}, phen-H_{c2}) 7.89-7.87, 7.78-

7.77 (t, 12H, phen-H_{d1}, phen-H_{d2}), 8.84-8.38, 7.95-7.91 (d, 12H, Ar - H₁, H₂), 6.86, 6.67-6.64 (d, 12H, Pz-H₄, H₃). Elemental analyses calcd (%) for C₁₂₆H₈₄N₃₂O₁₈Pd₆: C, 50.91; H, 2.85; N, 15.08; Found: C, 51.12; H, 2.91; N, 15.22.

The PF₆⁻ salt of **3** was obtained as yellow needle crystal in quantitative yield. ¹H NMR (400 MHz, CD₃CN , 25 °C): δ = 8.84-8.82, 8.76-8.74 (m, 12H, phen-H_{a1}, phen-H_{a2}), 8.61-8.60, 8.17-8.16 (m, 12H, phen-H_{b1}, phen-H_{b2}), 8.17, 8.16 (s, 12H, phen-H_{c1}, phen-H_{c2}) 7.96-7.93, 7.79-7.76 (t, 12H, phen-H_{d1}, phen-H_{d2}), 8.37-8.34, 7.96-7.94 (d, 12H, Ar-H₁, H₃), 6.86-6.84 (d, 12H, Pz-H₃, H₄). ¹³C NMR (100 MHz, CD₃CN, 25 °C, ppm): δ 152.05, 151.93, 151.66, 151.50, 148.27, 147.82, 147.01, 143.86, 141.68, 131.43, 128.74, 128.43, 128.31, 127.82, 126.80, 125.42, 124.85, 107.32. ESI-MS (CH₃CN, m/z): 549.24, 722.79, 1011.72, 1590.58 for [3]⁶⁺, [3·PF₆⁻]⁵⁺, [3·2PF₆⁻]⁴⁺, [3·3PF₆⁻]³⁺, [3·4PF₆⁻]²⁺. Elemental analyses calcd (%) for C₁₂₆H₈₄N₂₆F₃₆P₆Pd₆: C, 43.61; H, 2.44; N, 10.49; Found: C, 43.65; H, 2.41; N, 10.52.

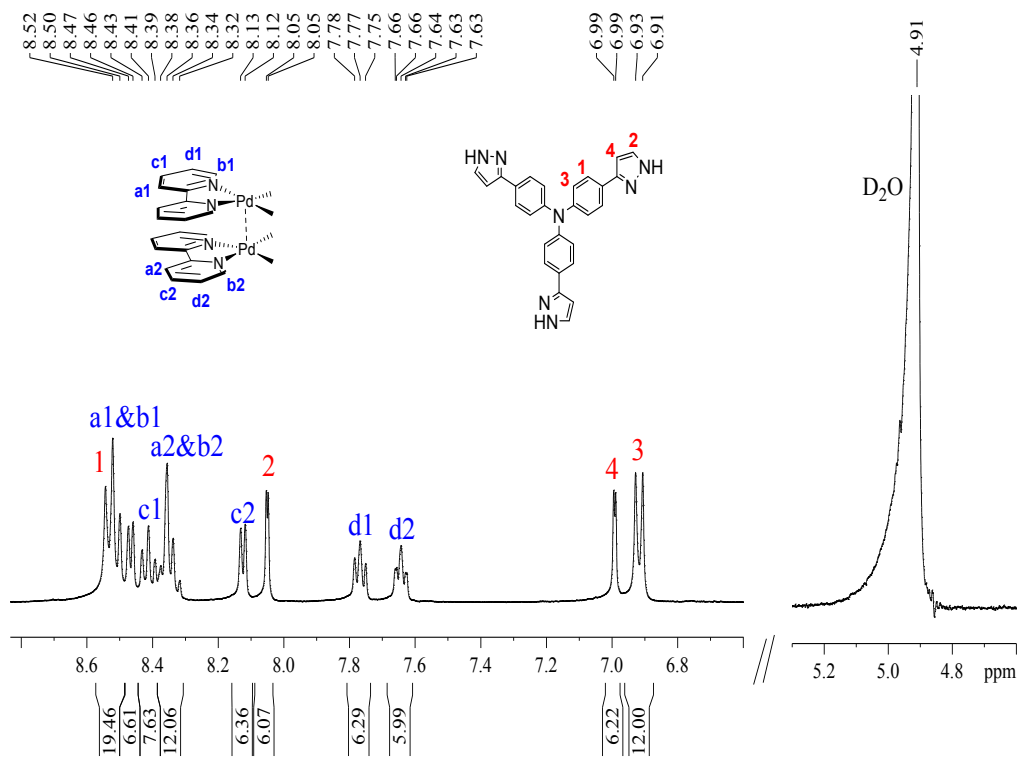


Fig. S1 The ¹H NMR spectrum of **1**·6NO₃⁻ in D₂O at 298 K.

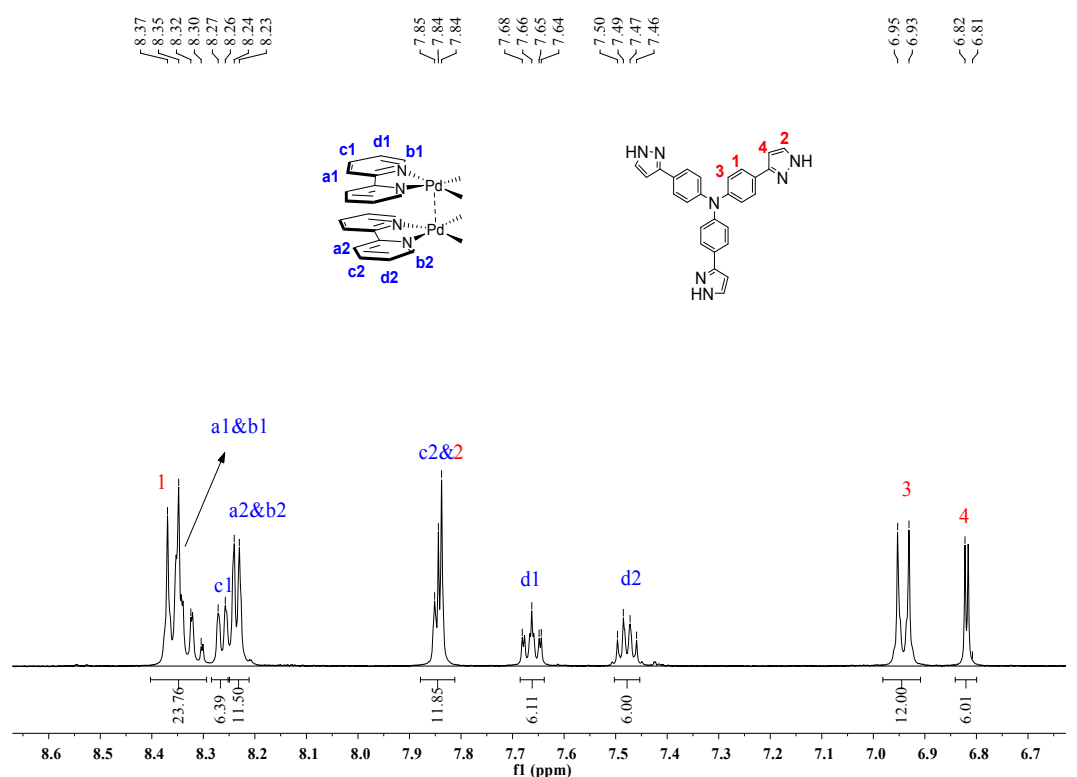


Fig. S2 The ^1H NMR spectrum of $\mathbf{1}\cdot 6\text{PF}_6^-$ in CD_3CN at 298 K.

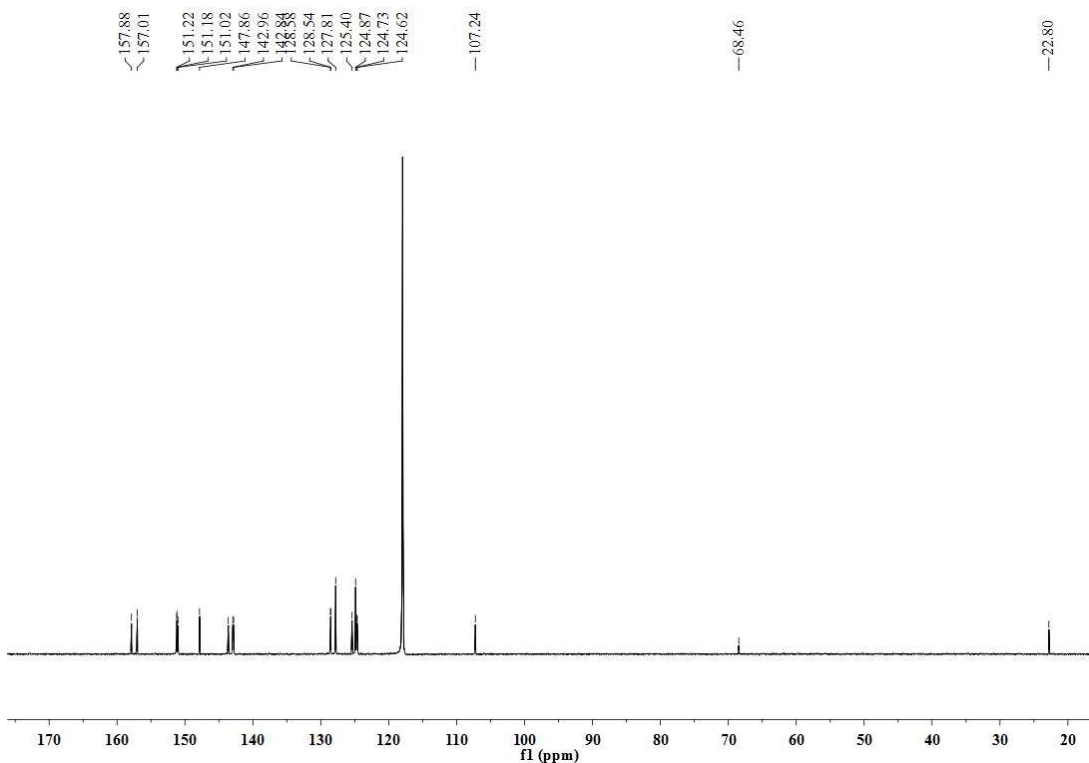


Fig. S3 The ^{13}C NMR spectrum of $\mathbf{1}\cdot 6\text{PF}_6^-$ in CD_3CN at 298 K.

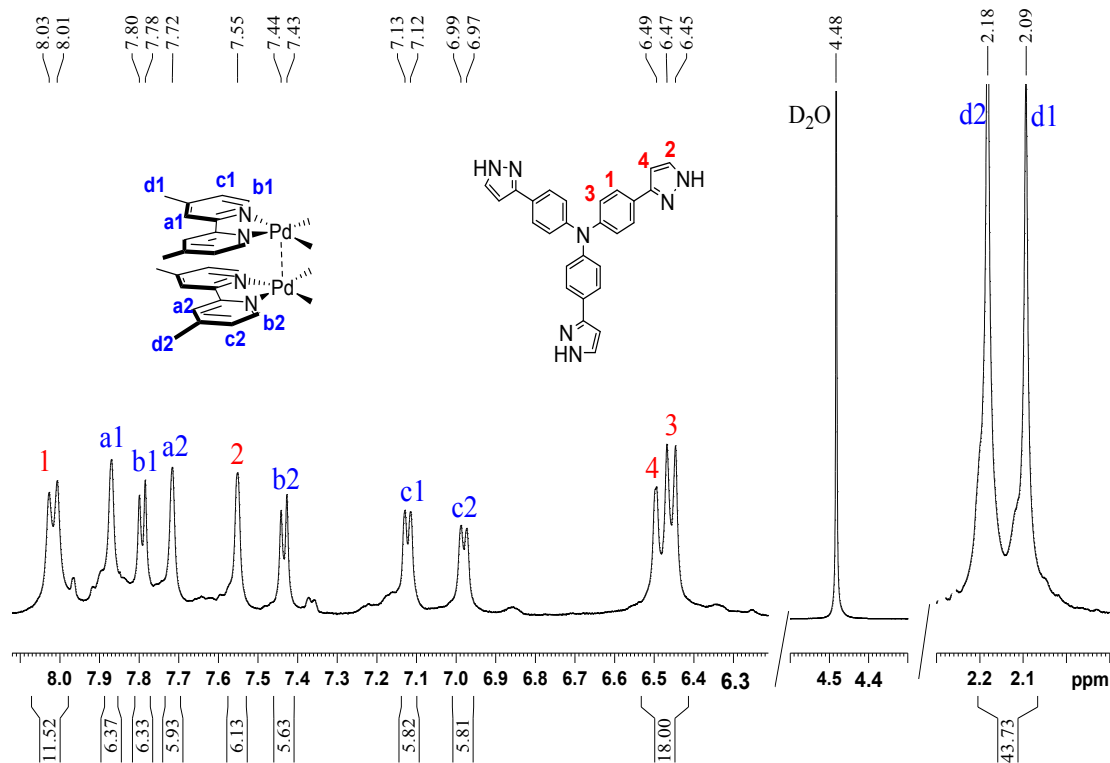


Fig. S4 The ¹H NMR spectrum of **2**·6NO₃⁻ in D₂O at 298 K.

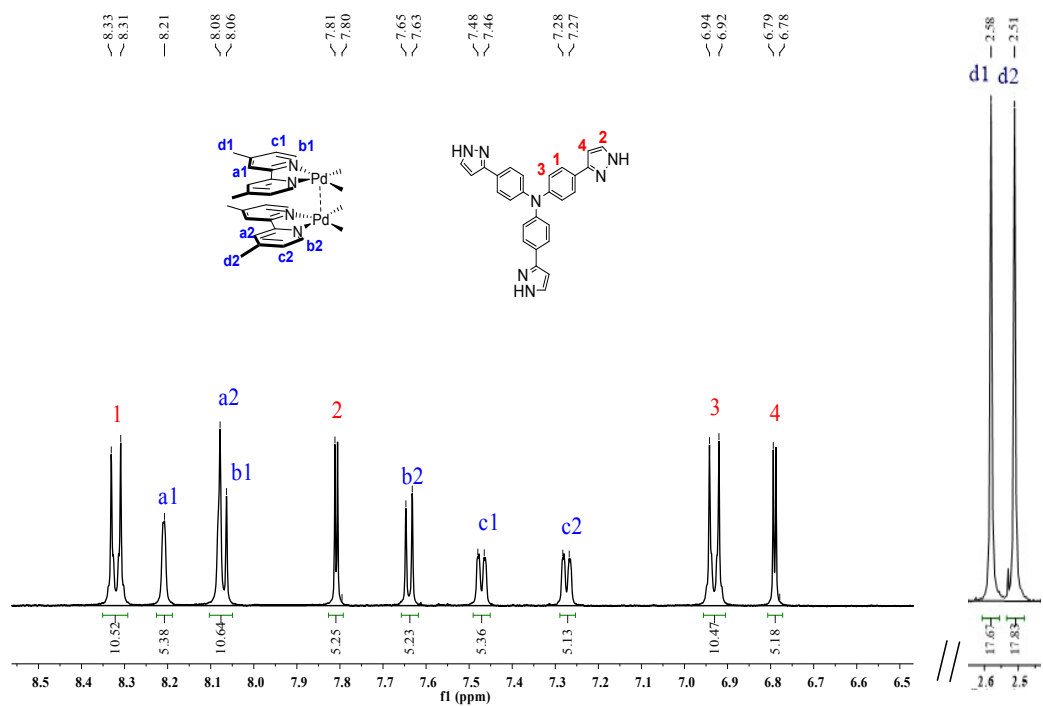


Fig. S5 The ¹H NMR spectrum of **2**·6PF₆⁻ in CD₃CN at 298 K.

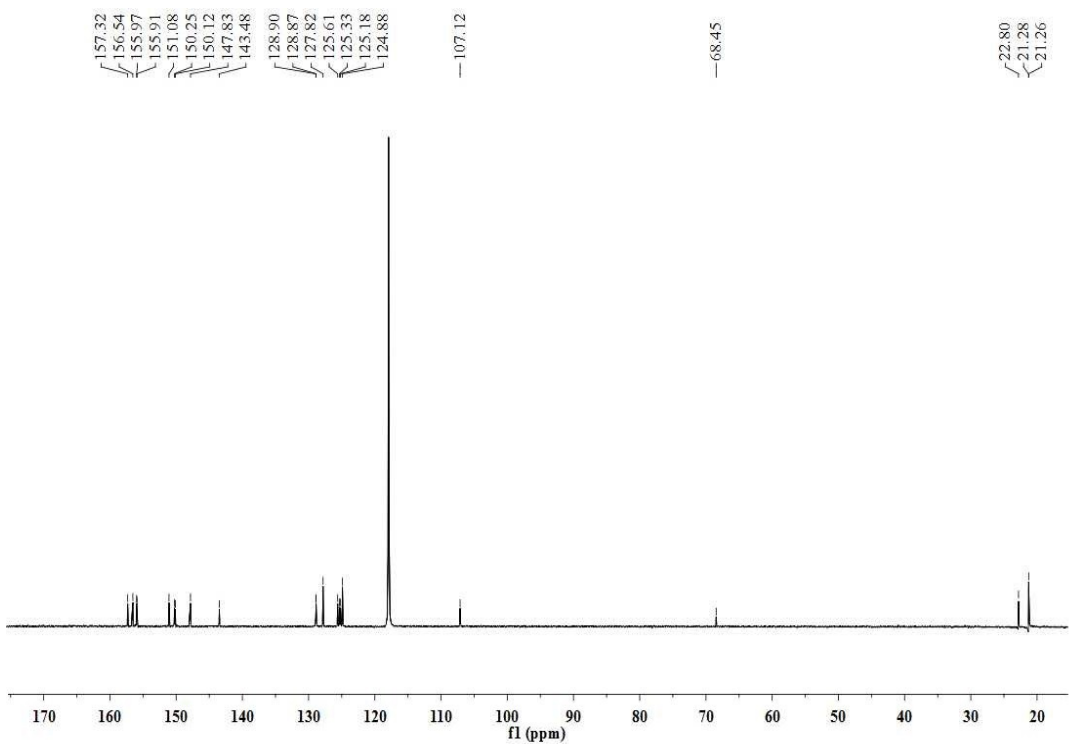


Fig. S6 The ^{13}C NMR spectrum of $\mathbf{2}\cdot\text{PF}_6^-$ in CD_3CN at 298 K.

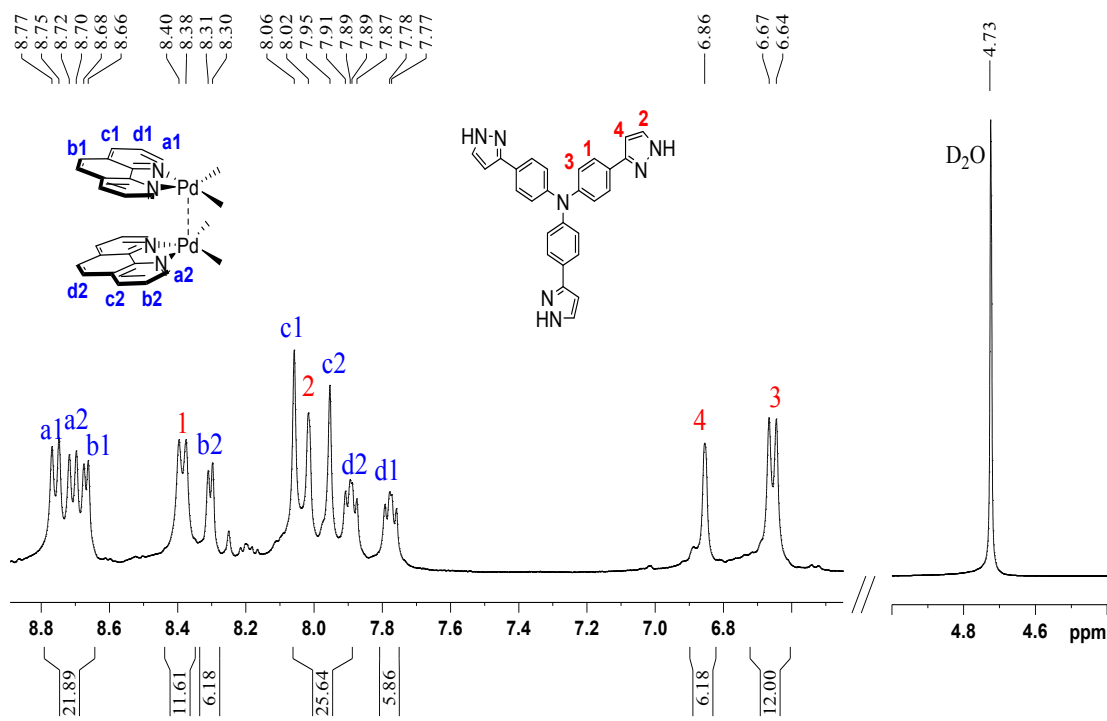


Fig. S7 The ^1H NMR spectrum of $\mathbf{3}\cdot 6\text{NO}_3^-$ in D_2O at 298K.

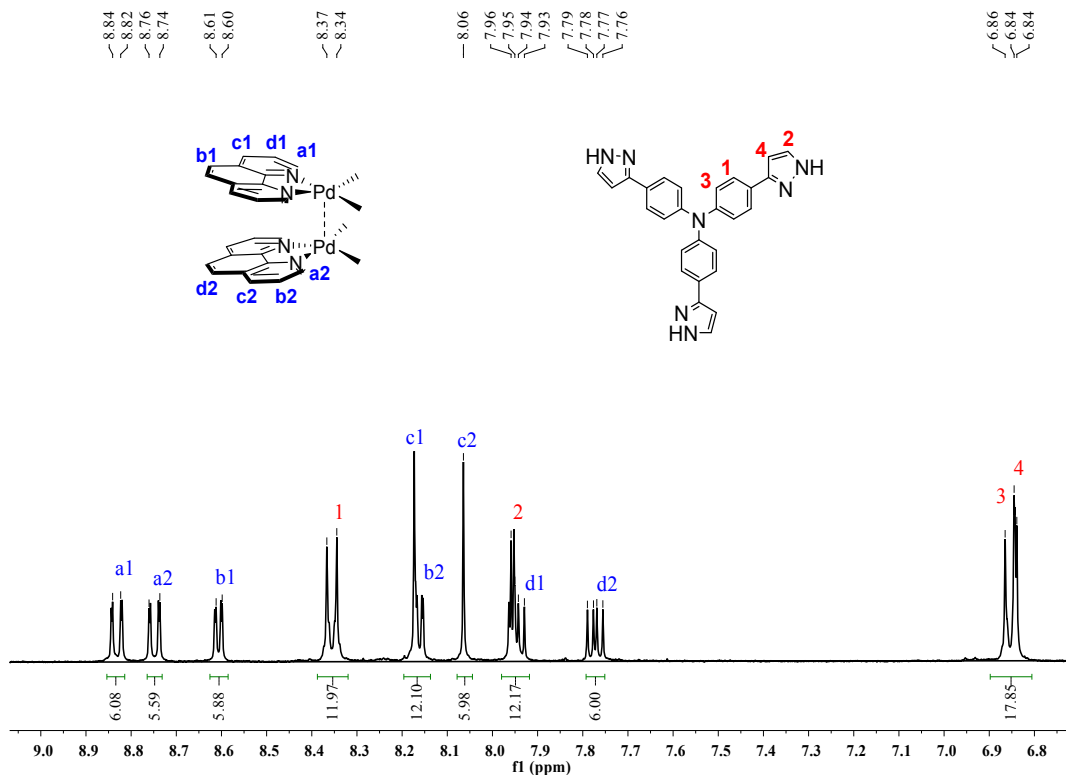


Fig. S8 The ¹H NMR spectrum of **3**·6PF₆⁻ in CD₃CN at 298 K.

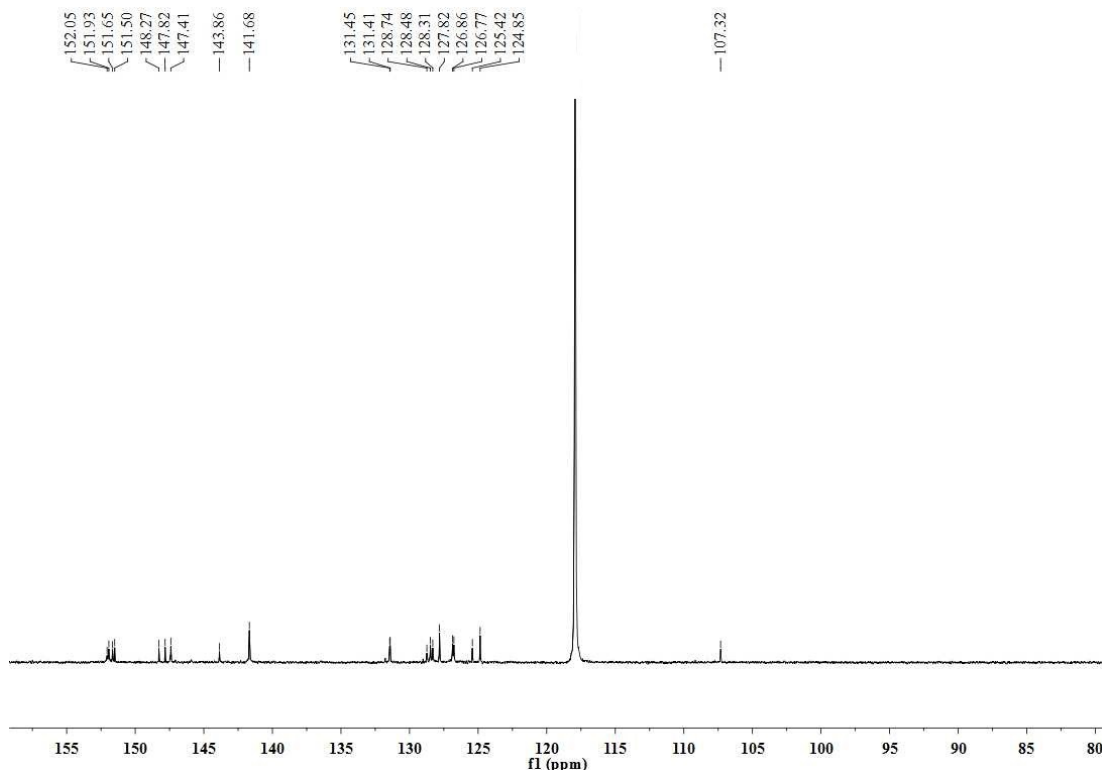


Fig. S9 The ¹³C NMR spectrum of **3**·6PF₆⁻ in CD₃CN at 298 K.

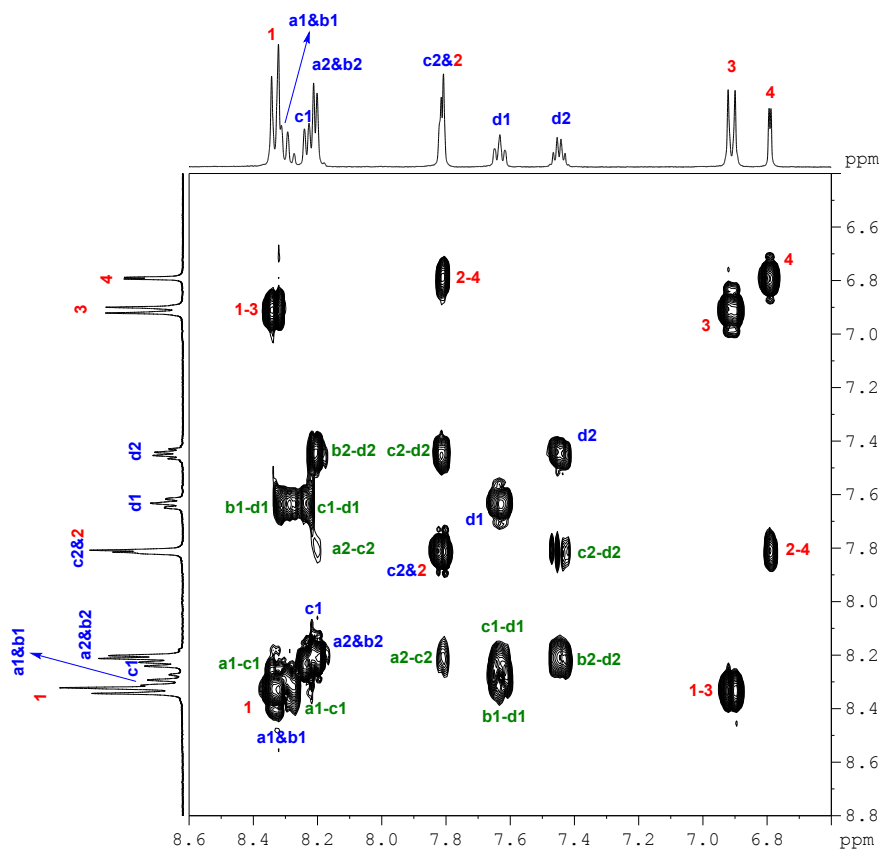


Fig. S10 The ^1H - ^1H COSY spectrum of $\mathbf{1}\cdot 6\text{PF}_6^-$ in CD_3CN at 298 K.

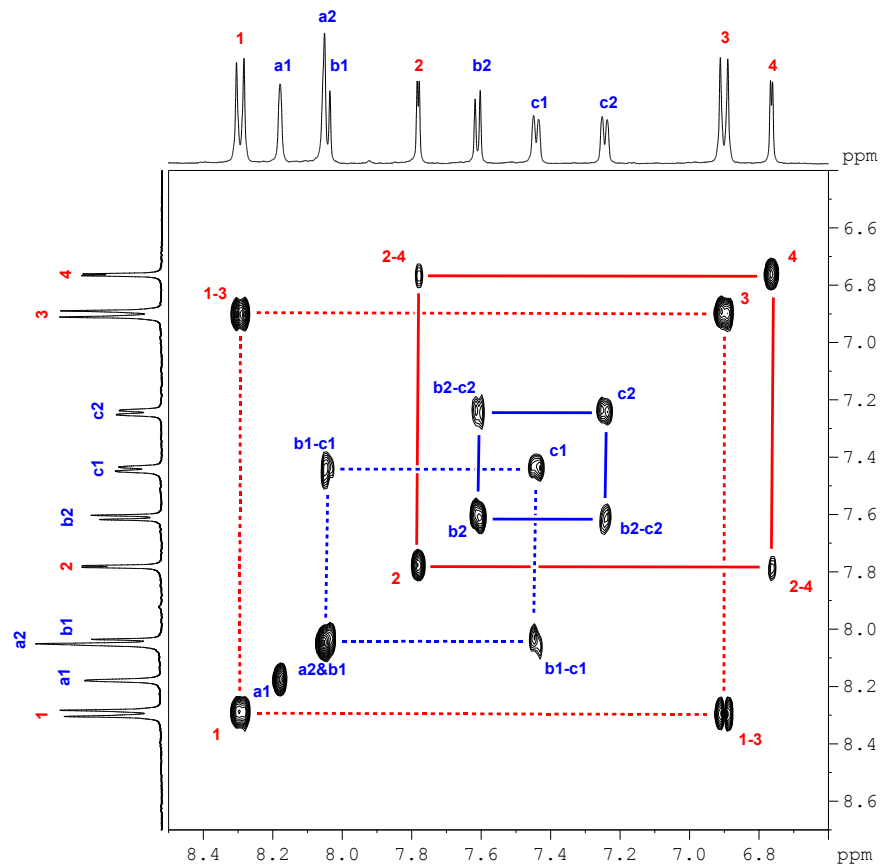


Fig. S11 The ^1H - ^1H COSY spectrum of $\mathbf{2}\cdot 6\text{PF}_6^-$ in CD_3CN at 298 K.

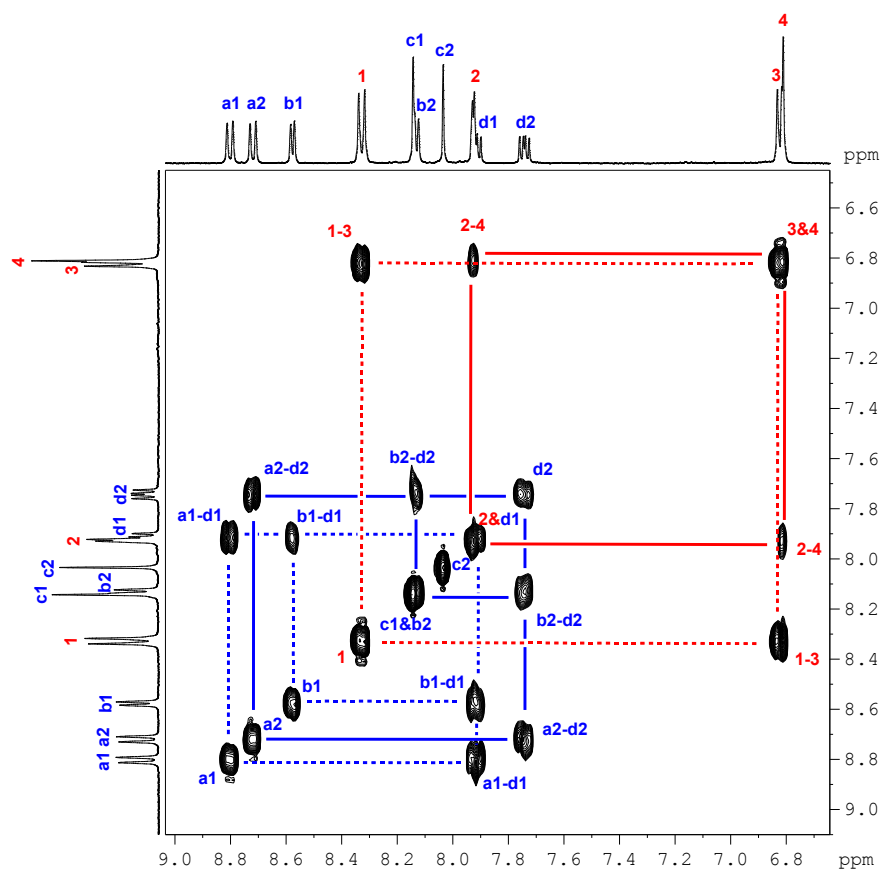


Fig. S12 The ^1H - ^1H COSY spectrum of $3 \cdot 6\text{PF}_6^-$ in CD_3CN at 298 K.

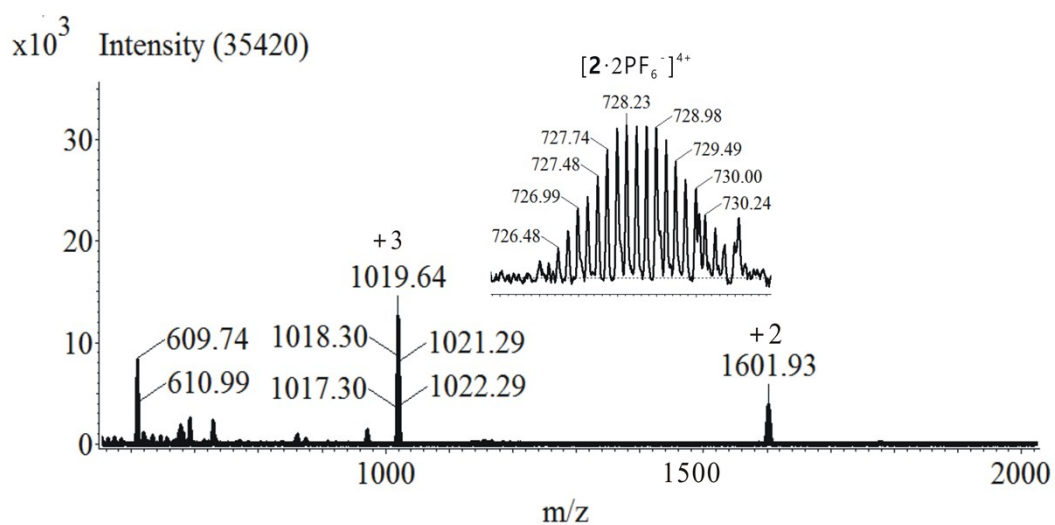


Fig. S13 ESI-MS spectra of $2\cdot6\text{PF}_6^-$ in CH_3CN ; the inset shows the isotopic distribution of the species $[2\cdot2\text{PF}_6^-]^{4+}$.

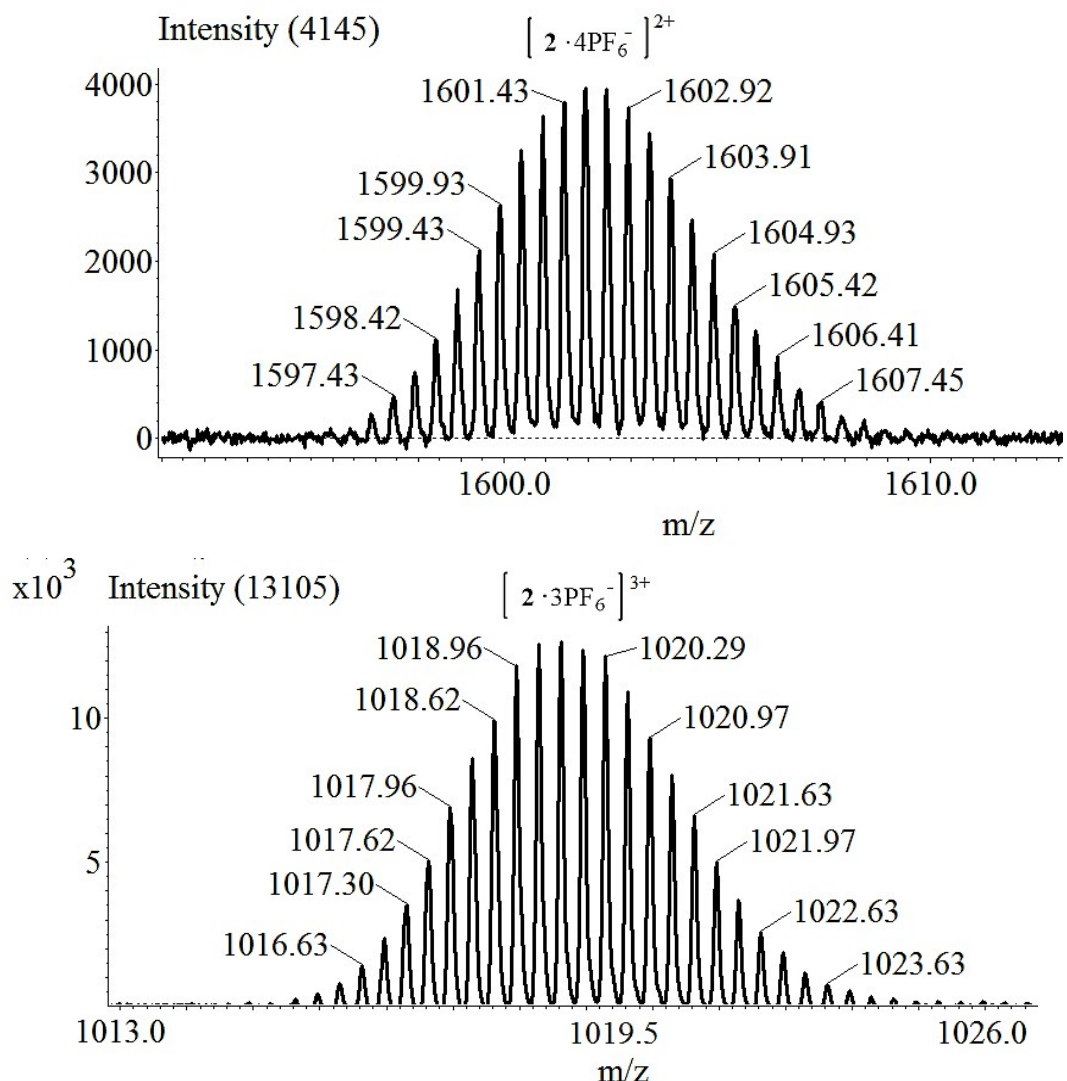


Fig. S14 ESI-MS spectra of $[2\cdot3\text{PF}_6^-]^{3+}$ and $[2\cdot4\text{PF}_6^-]^{2+}$ in CH_3CN .

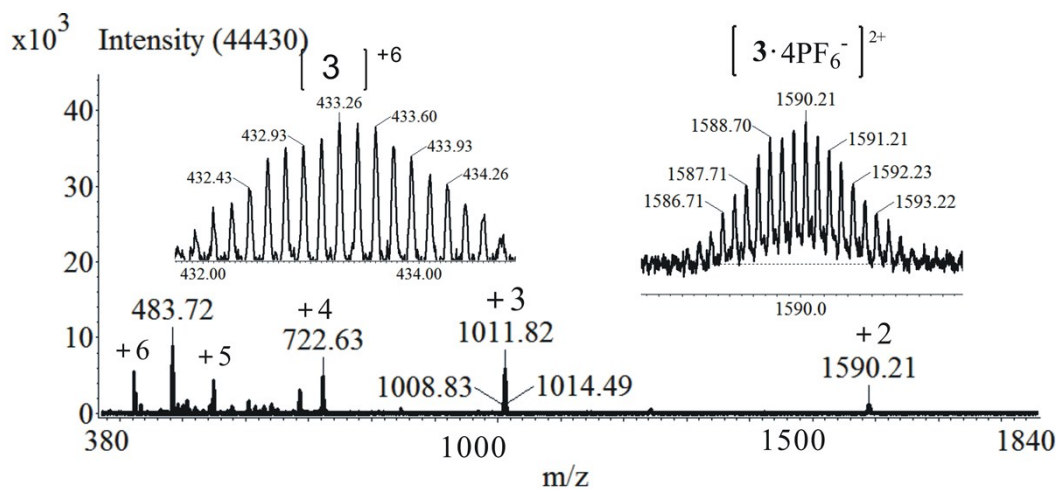
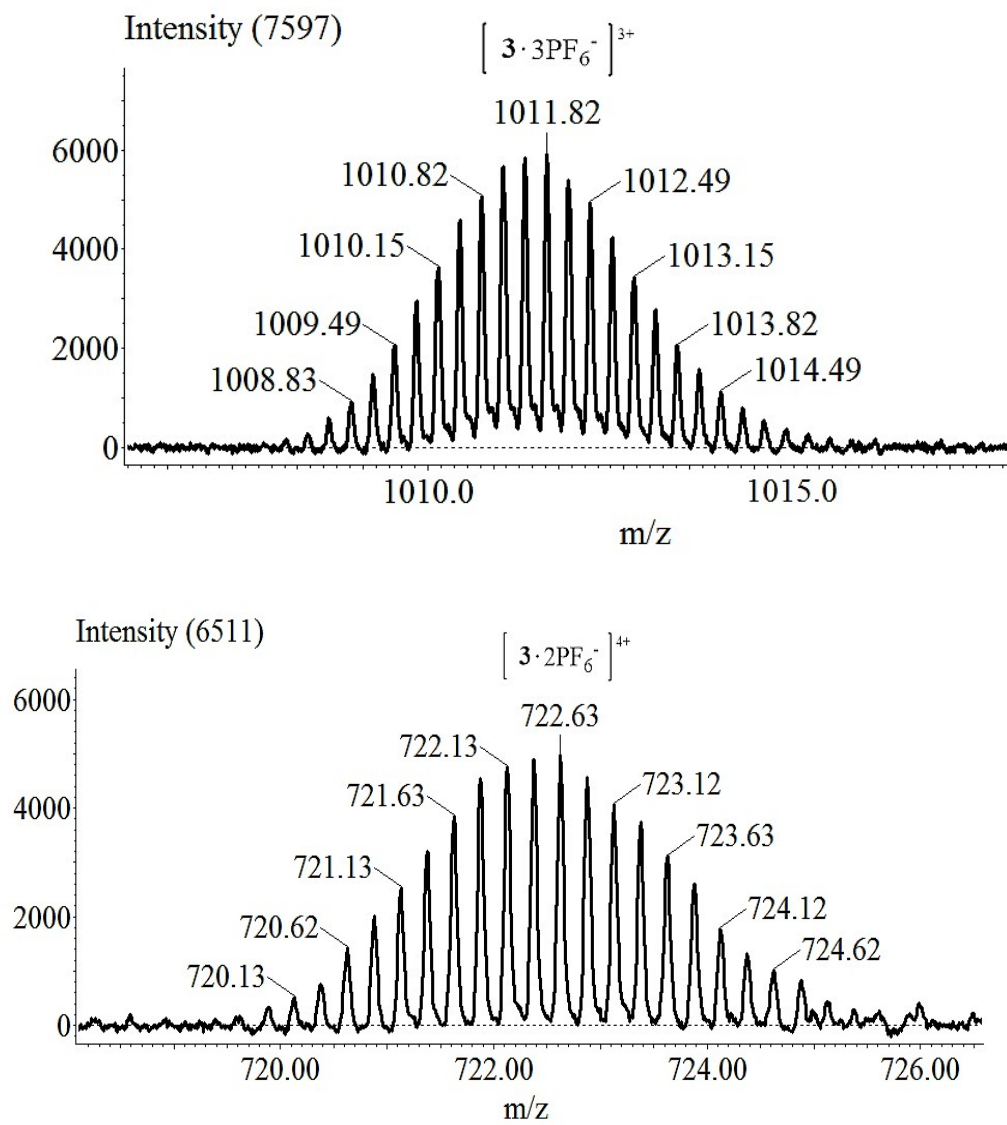


Fig. S15 ESI-MS spectra of $3 \cdot 6\text{PF}_6^-$ in CH_3CN ; the inset shows the isotopic distribution of the species $[3 \cdot 4\text{PF}_6^-]^{2+}$ and $[3]^{6+}$.



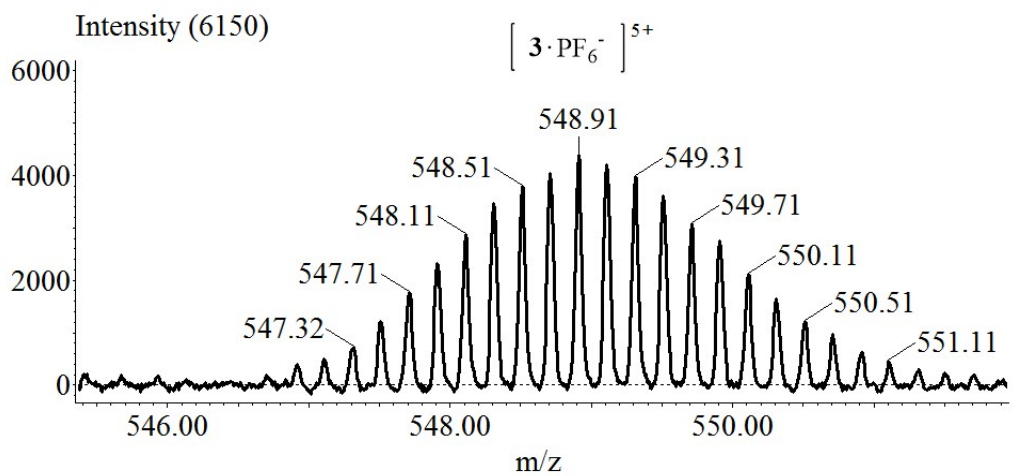


Fig. S16 ESI-MS spectra of $[\text{3} \cdot 3\text{PF}_6^-]^{3+}$, $[\text{3} \cdot 2\text{PF}_6^-]^{4+}$ and $[\text{3} \cdot \text{PF}_6^-]^{5+}$ in CH_3CN .

Table S1. Crystallographic data for complexes **1-3**.

	1·6PF₆⁻·10 CH₃CN	1/2(2·6PF₆⁻·2CH₃CN)	3·6PF₆⁻
Formula	C ₁₃₄ H ₁₁₄ F ₃₆ N ₃₆ P ₆ Pd ₆	C ₆₅ H ₅₆ F ₁₈ N ₁₄ P ₃ Pd ₃	C ₁₂₆ H ₈₄ N ₂₆ F ₃₆ P ₆ Pd ₆
FW	3736.83	1787.34	3470.41
crystal system	Monoclinic	Orthorhombic	Hexagonal
space group	P2 ₁ /c	Pnma	P6/m
a [Å]	18.712(4)	58.295(7)	29.983(4)
b [Å]	38.357(8)	11.9914(14)	29.983(4)
c [Å]	22.714(5)	24.911(3)	11.399(2)
α [°]	90	90	90
β [°]	110.07(3)	90	90
γ [°]	90	90	120
V [Å ³]	15313(6)	17414(4)	8875(3)
Z	4	8	2
ρcalcd, [g/cm ⁻³]	1.621	1.363	1.299
μ [mm ⁻¹]	0.812	0.749	0.732
F(000)	7440.0	7112.0	3424.0
2θmax [°]	51.36	50.70	51.36
no. unique data	30809	8031	4392
Parameters	2048	1064	350
GOF [F ²] ^a	1.038	1.020	1.035
R[F ² >2σ(F ²)],	0.0379	0.1171	0.0779
wR[F ²] ^b	0.1099	0.3293	0.2383

[a] GOF = [w(F_o²-F_c²)²]/(n - p)^{1/2}, where n and p denote the number of data points and the number of parameters, respectively. [b] R1 = (||F_o|| - |F_c|)/|F_o|; wR2 =[w(F_o²-F_c²)²]/[w(F_o²)²]^{1/2}, Where w=1/[σ²(F_o²)+(aP)²+bP] and P=[max(0,F_o²)+2F_c²]/3.

Table S2. Selected bond distances (Å) and angles (°) of complex **1**·6PF₆⁻.

Bond Dist.[Å]	Bond Dist.[Å]
Pd(1)-N(1)	1.999(3)
Pd(1)-N(4)	2.004(3)
Pd(1)-N(25)	2.006(3)
Pd(1)-N(26)	2.009(3)
Pd(2)-N(2)	2.032(3)
Pd(2)-N(23)	2.022(3)
Pd(2)-N(24)	2.021(3)
Pd(2)-N(3)	2.021(3)
Pd(3)-N(7)	1.999(3)
Pd(3)-N(6)	2.041(3)
Pd(3)-N(21)	2.013(3)
Pd(3)-N(22)	2.019(3)
Pd(4)-N(8)	2.012(3)
Pd(4)-N(11)	2.011(3)
Pd(4)-N(10)	2.006(3)
Pd(4)-N(9)	2.006(5)
Pd(5)-N(19)	2.025(3)
Pd(5)-N(13)	2.017(5)
Pd(5)-N(14)	2.014(3)
Pd(5)-N(20)	2.011(3)
Pd(6)-N(15)	2.016(3)
Pd(6)-N(17)	2.002(3)
Pd(6)-N(18)	2.008(3)
Pd(6)-N(16)	1.996(3)
N(2)-N(1)	1.381(4)
N(4)-N(3)	1.358(4)
N(6)-N(9)	1.381(4)
N(7)-N(8)	1.367(4)
N(13)-N(16)	1.364(4)
N(14)-N(15)	1.365(4)
Pd(1)-Pd(2)	3.1596(7)
Pd(3)-Pd(4)	3.0833(7)
Pd(6)-Pd(5)	3.1266(6)
Bond Angel[°]	Bond Angel[°]
N(1)-Pd(1)-Pd(2)	62.34(8)
N(1)-Pd(1)-N(4)	87.11(11)
N(1)-Pd(1)-N(25)	95.29(11)
N(1)-Pd(1)-N(26)	176.51(12)
N(4)-Pd(1)-Pd(2)	62.60(7)
N(4)-Pd(1)-N(26)	96.30(13)
N(25)-Pd(1)-Pd(2)	119.71(8)
N(25)-Pd(1)-N(4)	177.27(11)
N(25)-Pd(1)-N(26)	81.28(12)
N(26)-Pd(1)-Pd(2)	119.96(10)
N(2)-Pd(2)-Pd(1)	65.12(7)
N(23)-Pd(2)-Pd(1)	109.91(8)
N(23)-Pd(2)-N(2)	174.00(10)
N(24)-Pd(2)-Pd(1)	113.99(8)
N(24)-Pd(2)-N(2)	97.80(11)
N(24)-Pd(2)-N(23)	81.00(11)
N(3)-Pd(2)-Pd(1)	64.14(7)
N(3)-Pd(2)-N(2)	85.63(11)
N(3)-Pd(2)-N(23)	95.21(11)
N(3)-Pd(2)-N(24)	175.00(11)
N(7)-Pd(3)-Pd(4)	65.08(8)
N(8)-Pd(4)-Pd(3)	64.25(7)
N(11)-Pd(4)-Pd(3)	119.20(8)
N(11)-Pd(4)-N(8)	97.04(12)
N(10)-Pd(4)-Pd(3)	112.48(8)
N(10)-Pd(4)-N(8)	175.07(11)
N(10)-Pd(4)-N(11)	81.28(12)
N(9)-Pd(4)-Pd(3)	63.95(8)
N(9)-Pd(4)-N(8)	86.38(12)
N(9)-Pd(4)-N(11)	176.12(11)
N(9)-Pd(4)-N(10)	95.46(12)
N(19)-Pd(5)-Pd(6)	118.52(7)
N(19)-Pd(5)-N(14)	99.79(11)
N(13)-Pd(5)-Pd(6)	63.68(7)
N(13)-Pd(5)-N(19)	174.80(11)
N(13)-Pd(5)-N(14)	85.40(11)
N(14)-Pd(5)-Pd(6)	63.68(7)
N(20)-Pd(5)-Pd(6)	111.27(8)
N(20)-Pd(5)-N(19)	80.89(11)
N(20)-Pd(5)-N(13)	93.93(11)
N(20)-Pd(5)-N(14)	175.77(10)
N(15)-Pd(6)-Pd(5)	63.19(8)

N(7)-Pd(3)-N(6)	84.82(11)	N(17)-Pd(6)-Pd(5)	112.16(8)
N(7)-Pd(3)-N(21)	96.04(11)	N(17)-Pd(6)-N(15)	172.50(12)
N(7)-Pd(3)-N(22)	174.12(11)	N(17)-Pd(6)-N(18)	81.07(12)
N(6)-Pd(3)-Pd(4)	66.11(7)	N(18)-Pd(6)-Pd(5)	118.03(8)
N(21)-Pd(3)-Pd(4)	110.79(7)	N(18)-Pd(6)-N(15)	95.83(12)
N(21)-Pd(3)-N(6)	176.09(11)	N(16)-Pd(6)-Pd(5)	63.19(8)
N(21)-Pd(3)-N(22)	81.18(11)	N(16)-Pd(6)-N(15)	86.91(12)
N(22)-Pd(3)-Pd(4)	110.96(9)	N(16)-Pd(6)-N(17)	96.20(12)
N(22)-Pd(3)-N(6)	97.61(11)	N(16)-Pd(6)-N(18)	177.26(12)

Table S3. Selected bond distances (Å) and angles (°) of complex **2**·6PF₆⁻.

Bond Dist.[Å]	Bond Dist.[Å]
Pd(1)-N(1)	1.996(11)
Pd(1)-N(1)#1	1.995(11)
Pd(1)-N(8)#1	2.006(11)
Pd(1)-N(8)	2.006(11)
Pd(2)-N(2)	2.011(11)
Pd(2)-N(2)#1	2.011(11)
Pd(2)-N(9)	2.017(11)
Pd(2)-N(9)#1	2.017(11)
Pd(3)-N(3)	1.980(16)
Pd(3)-N(3)#1	1.980(16)
Pd(3)-N(10)	1.983(17)
Pd(3)-N(10)#1	1.983(17)
Pd(4)-N(4)#1	1.987(14)
Pd(4)-N(4)	1.987(14)
Pd(4)-N(11)#1	2.015(13)
Pd(4)-N(11)	
Pd(5)-N(11)	2.015(13)
Pd(5)-N(5)#1	1.997(10)
Pd(5)-N(5)	1.997(10)
Pd(5)-N(12)	2.006(10)
Pd(5)-N(12)#1	2.006(10)
Pd(6)-N(6)	2.007(10)
Pd(6)-N(6)#1	2.007(10)
Pd(6)-N(13)#1	2.004(10)
Pd(6)-N(13)	2.004(10)
N(1)-N(2)	1.374(13)
N(3)-N(4)	1.387(16)
N(5)-N(6)	1.380(12)
Pd(1)-Pd(2)	3.144(2)
Pd(3)-Pd(4)	3.161(2)
Pd(5)-Pd(6)	3.1510(19)
Bond Angel[°]	Bond Angel[°]
N(1)#1-Pd(1)-Pd(2)	62.9(3)
N(1)-Pd(1)-Pd(2)	62.9(3)
N(1)#1-Pd(1)-N(1)	87.2(7)
N(1)-Pd(1)-N(8)#1	176.9(5)
N(1)#1-Pd(1)-N(8)#1	95.9(5)
N(1)#1-Pd(1)-N(8)	176.9(5)
N(1)-Pd(1)-N(8)	95.9(5)
N(8)-Pd(1)-Pd(2)	118.6(3)
N(8)#1-Pd(1)-Pd(2)	118.6(3)
N(8)#1-Pd(1)-N(8)	81.0(7)
N(2)-Pd(2)-Pd(1)	64.5(3)
N(2)#1-Pd(2)-Pd(1)	64.5(3)
N(2)-Pd(2)-N(2)#1	83.8(6)
N(2)#1-Pd(2)-N(9)#1	98.2(4)
N(2)-Pd(2)-N(9)	98.2(4)
N(2)#1-Pd(2)-N(9)	176.4(4)
N(2)-Pd(2)-N(9)#1	176.4(4)
N(9)-Pd(2)-Pd(1)	113.6(3)
N(9)#1-Pd(2)-Pd(1)	113.6(3)
N(9)-Pd(2)-N(9)#1	79.7(6)
N(3)#1-Pd(3)-Pd(4)	62.2(4)
N(3)-Pd(3)-Pd(4)	62.2(4)
N(4)#1-Pd(4)-Pd(3)	64.5(4)
N(4)-Pd(4)-Pd(3)	64.5(4)
N(4)#1-Pd(4)-N(4)	85.0(9)
N(4)-Pd(4)-N(11)	176.6(5)
N(4)#1-Pd(4)-N(11)	96.6(6)
N(4)#1-Pd(4)-N(11)#1	176.6(5)
N(4)-Pd(4)-N(11)#1	96.6(6)
N(11)#1-Pd(4)-Pd(3)	113.4(3)
N(11)-Pd(4)-Pd(3)	113.4(3)
N(11)-Pd(4)-N(11)#1	81.6(7)
N(5)-Pd(5)-Pd(6)	63.0(3)
N(5)#1-Pd(5)-Pd(6)	63.0(3)
N(5)-Pd(5)-N(5)#1	86.6(6)
N(5)#1-Pd(5)-N(12)	95.8(4)
N(5)-Pd(5)-N(12)#1	95.8(4)
N(5)#1-Pd(5)-N(12)#1	177.1(4)
N(5)-Pd(5)-N(12)	177.1(4)
N(12)#1-Pd(5)-Pd(6)	116.8(3)
N(12)-Pd(5)-Pd(6)	116.8(3)
N(12)#1-Pd(5)-N(12)	81.7(6)
N(6)#1-Pd(6)-Pd(5)	64.4(3)
N(6)-Pd(6)-Pd(5)	64.4(3)

N(3)#1-Pd(3)-N(3)	86.3(9)	N(6)#1-Pd(6)-N(6)	85.3(6)
N(3)#1-Pd(3)-N(10)#1	96.0(7)	N(13)-Pd(6)-Pd(5)	115.9(3)
N(3)-Pd(3)-N(10)#1	177.7(7)	N(13)#1-Pd(6)-Pd(5)	115.9(3)
N(3)#1-Pd(3)-N(10)	177.7(7)	N(13)#1-Pd(6)-N(6)#1	177.8(4)
N(3)-Pd(3)-N(10)	96.0(7)	N(13)-Pd(6)-N(6)#1	96.8(4)
N(10)#1-Pd(3)-Pd(4)	119.0(4)	N(13)#1-Pd(6)-N(6)	96.8(4)
N(10)-Pd(3)-Pd(4)	119.0(4)	N(13)-Pd(6)-N(6)	177.8(4)
N(10)-Pd(3)-N(10)#1	81.7(10)	N(13)#1-Pd(6)-N(13)	81.1(6)

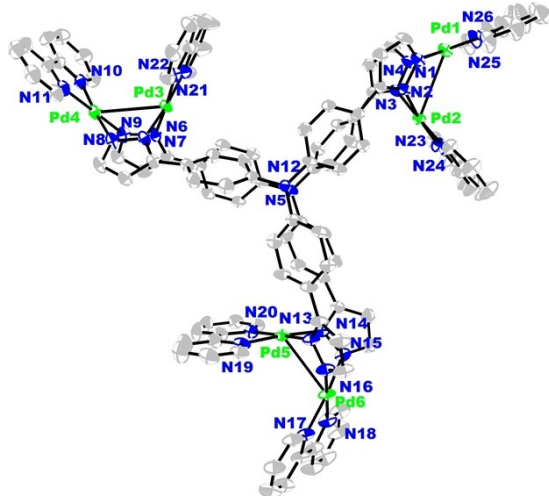
Symmetry transformations used to generate equivalent atoms: #1 x,-y+1/2,z

Table S4. Selected bond distances (Å) and angles (°) of complex **3**·6PF₆⁻.

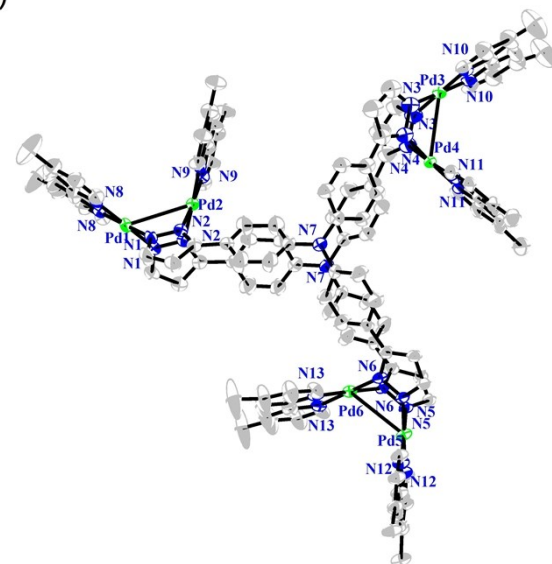
Bond Dist.[Å]	Bond Dist.[Å]
Pd(1)-Pd(2)	3.2963(11)
Pd(1)-N(5)#1	2.024(6)
Pd(1)-N(5)	2.024(6)
Pd(1)-N(1)	2.004(6)
Pd(1)-N(1)#1	2.004(6)
Pd(2)-N(3)#1	2.027(6)
Pd(2)-N(3)	2.027(6)
Pd(2)-N(2)	2.006(6)
Pd(2)-N(2)#1	2.006(6)
N(5)-C(20)	1.39(2)
N(5)-C(16)	1.392(10)
N(5)-C(20A)	1.23(2)
N(3)-C(5)	1.294(11)
N(3)-C(1)	1.370(10)
N(2)-N(1)	1.374(8)
N(2)-C(7)	1.325(10)
N(1)-C(9)	1.337(9)
N(4)-C(13)#2	1.421(6)
N(4)-C(13)	1.421(6)
N(4)-C(13)#3	1.421(6)
Bond Angel[°]	Bond Angel[°]
N(5)#1-Pd(1)-Pd(2)	117.19(18)
N(5)-Pd(1)-Pd(2)	117.19(18)
N(5)#1-Pd(1)-N(5)	82.3(4)
N(1)#1-Pd(1)-Pd(2)	62.71(16)
N(1)-Pd(1)-Pd(2)	62.71(16)
N(1)-Pd(1)-N(5)#1	177.7(3)
N(1)#1-Pd(1)-N(5)	177.7(3)
N(1)#1-Pd(1)-N(5)#1	95.7(3)
N(1)-Pd(1)-N(5)	95.7(3)
N(1)-Pd(1)-N(1)#1	86.3(3)
N(3)#1-Pd(2)-Pd(1)	125.00(18)
N(3)-Pd(2)-Pd(1)	125.00(18)
N(3)-Pd(2)-N(3)#1	81.7(4)
N(2)#1-Pd(2)-Pd(1)	59.76(17)
N(2)-Pd(2)-Pd(1)	59.76(17)
N(2)#1-Pd(2)-N(3)	94.5(3)
N(2)#1-Pd(2)-N(3)#1	175.1(2)
N(2)-Pd(2)-N(3)	94.5(3)
N(2)-N(3)-Pd(1)	121.9(5)
C(7)-N(2)-Pd(2)	128.0(5)
C(7)-N(2)-N(1)	108.9(6)
N(2)-N(1)-Pd(1)	115.0(4)
C(9)-N(1)-Pd(1)	137.0(5)

Symmetry transformations used to generate equivalent atoms: #1 x,y,-z+2

(a)



(b)



(c)

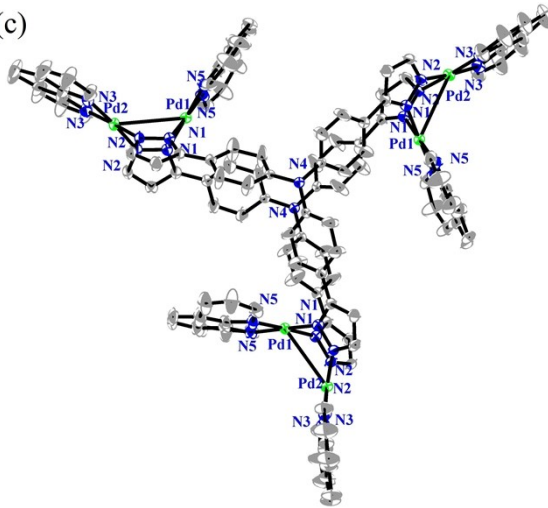


Fig. S17 The molecular structure of cations of **1**, **2**, **3**. The counterions, hydrogen atoms and solvent molecules are omitted for clarity.

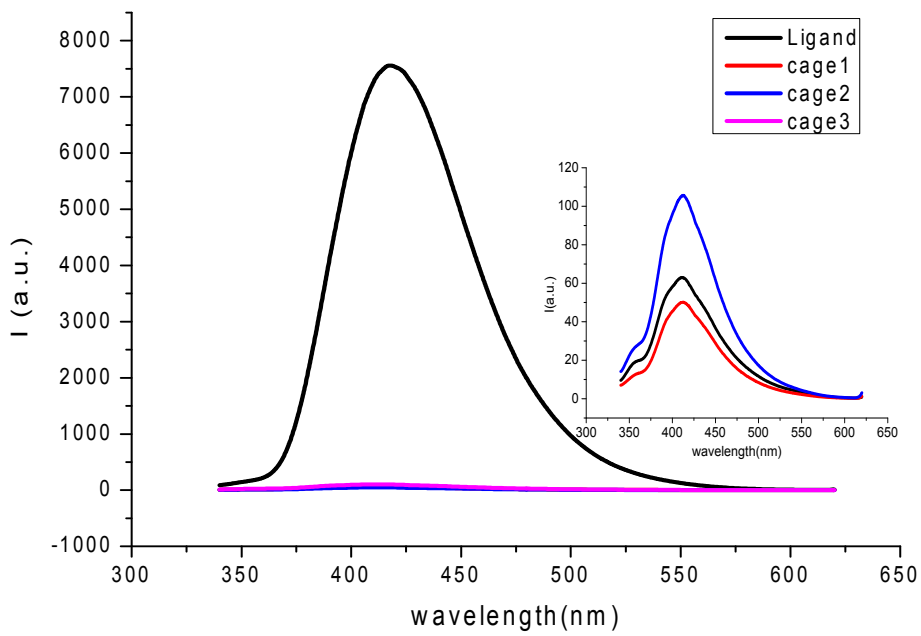


Fig. S18 Fluorescence emission spectra of H_3L and $\mathbf{1}\cdot 6\text{PF}_6^-$, $\mathbf{2}\cdot 6\text{PF}_6^-$, $\mathbf{3}\cdot 6\text{PF}_6^-$ in $\text{DMSO}/\text{H}_2\text{O}$ ((1:2, v/v) $\lambda_{\text{ex}} = 320$ nm).

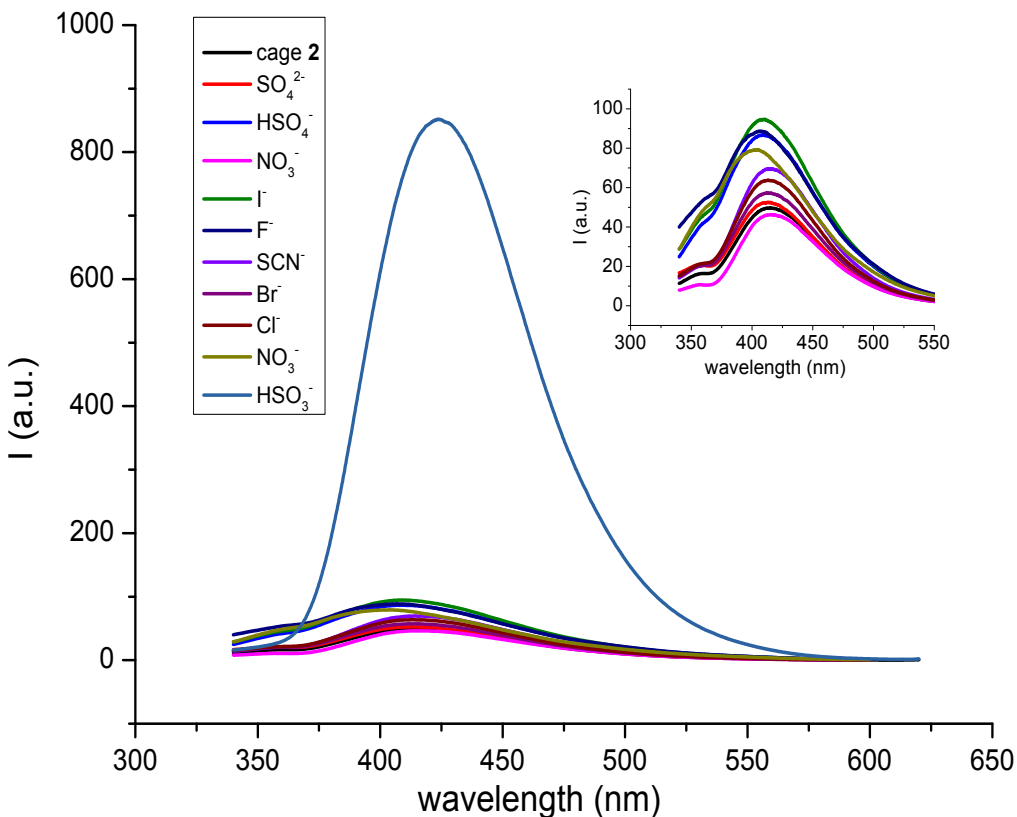


Fig. S19 Changes in fluorescent intensity for cage 2 (1.0×10^{-5} M) in $\text{CH}_3\text{CN}/\text{H}_2\text{O}$ (1:2, v/v) upon addition of different anions (Na^+ salts in H_2O).

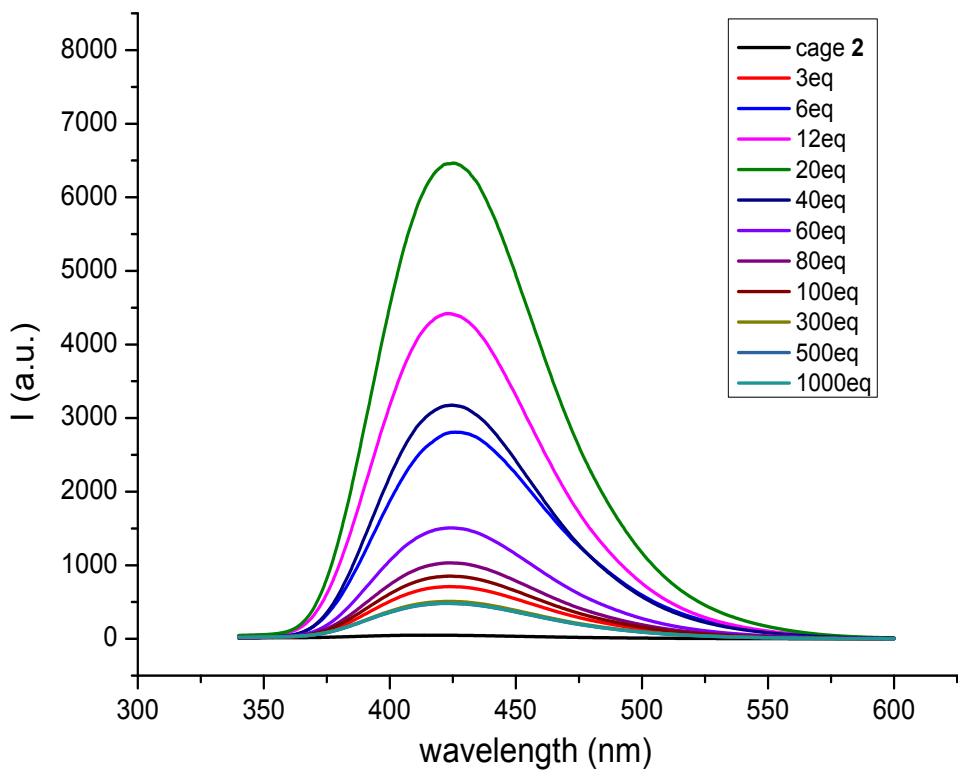


Fig. S20 Change in fluorescent intensity for cage 2 (1.0×10^{-5} M) in $\text{CH}_3\text{CN}/\text{H}_2\text{O}$ (1:2, v/v) after addition of various concentration of HSO_3^- anions (Na^+ salts in H_2O).

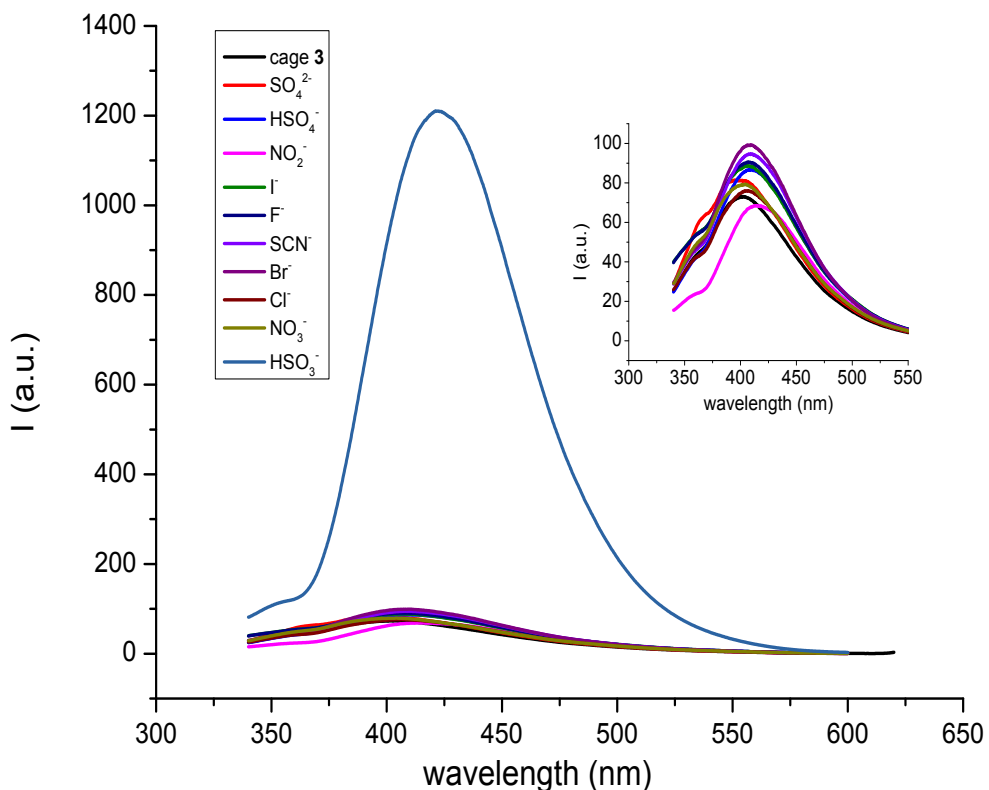


Fig. S21 Changes in fluorescent intensity for cage 3 (1.0×10^{-5} M) in $\text{CH}_3\text{CN}/\text{H}_2\text{O}$ (1:2, v/v) upon addition of different anions (Na^+ salts in H_2O).

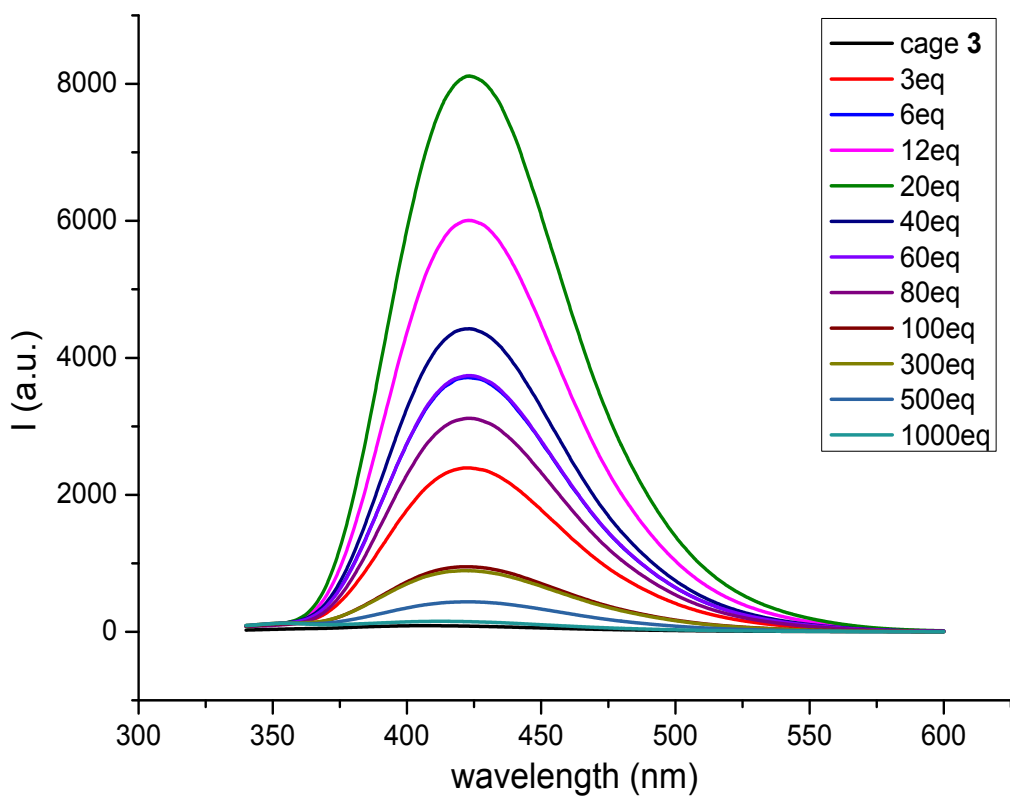


Fig. S22 Change in fluorescent intensity for cage **3**(1.0×10^{-5} M) in CH₃CN/H₂O (1:2, v/v) after addition of various concentration of HSO₄⁻ anions (Na⁺ salts in H₂O).

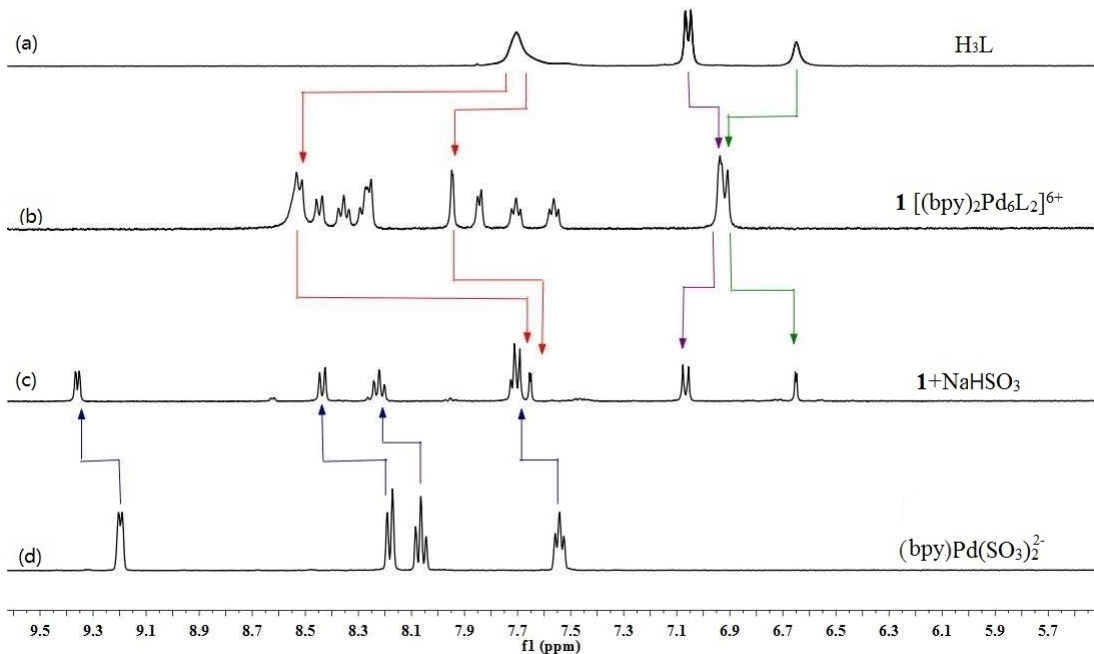


Fig. S23 ^1H NMR spectra of H_3L (a), $[(\text{bpy})_2\text{Pd}_6\text{L}_2]^{6+}$ (cage 1) (b), cage 1 + NaHSO_3 (c) and $(\text{bpy})\text{Pd}(\text{SO}_3)_2^{2-}$ (d) in $\text{DMSO-d}_6/\text{D}_2\text{O}$ (1:2, v/v).

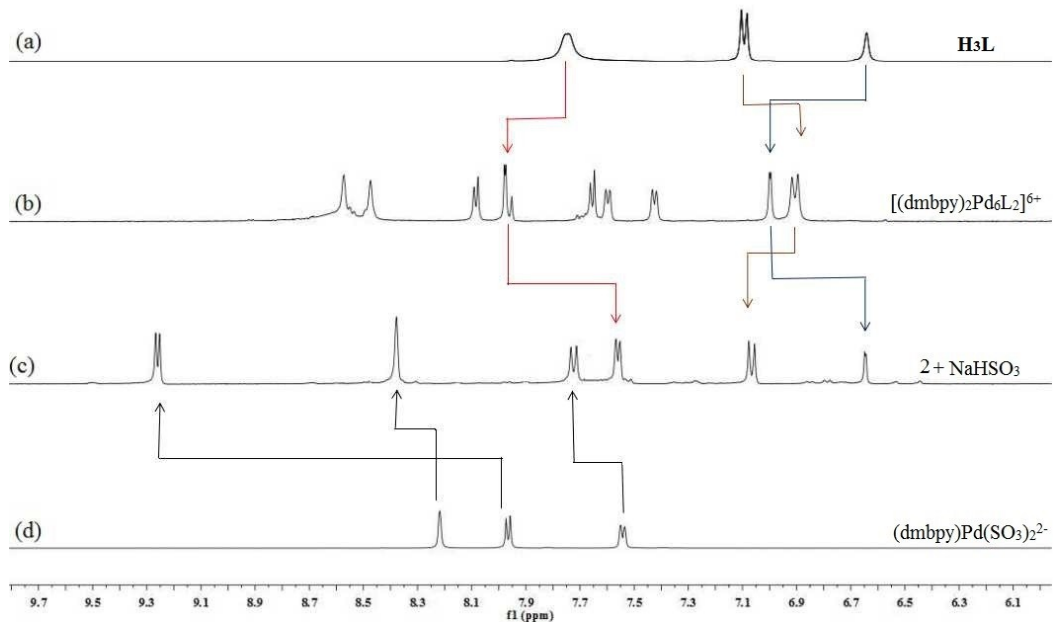


Fig. S24 ^1H NMR spectra of H_3L (a), $[(\text{dmbpy})_2\text{Pd}_6\text{L}_2]^{6+}$ (cage 2) (b), cage 2 + NaHSO_3 (c) and $(\text{dmbpy})\text{Pd}(\text{SO}_3)_2^{2-}$ (d) in $\text{DMSO-d}_6/\text{D}_2\text{O}$ (1:2, v/v).

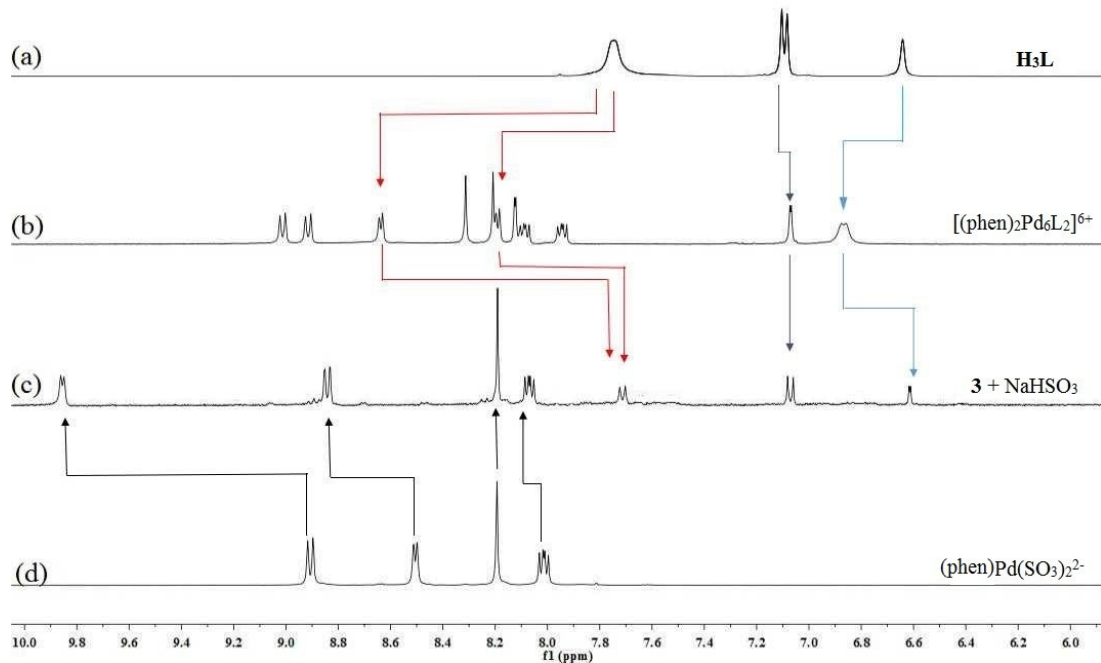


Fig. S25 ^1H NMR spectra of H_3L (a), $[(\text{phen})_2\text{Pd}_6\text{L}_2]^{6+}$ (cage **3**) (b), cage **3** + NaHSO_3 (c) and $(\text{phen})\text{Pd}(\text{SO}_3)_2^{2-}$ (d) in $\text{DMSO-d}_6/\text{D}_2\text{O}$ (1:2, v/v).

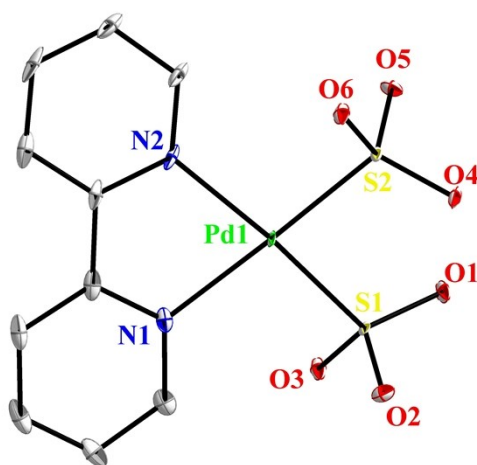


Fig. S26 The molecular structure of anion of $(\text{bpy})\text{Pd}(\text{SO}_3)_2^{2-}$. The counterions, hydrogen atoms and solvent molecules are omitted for clarity. The selected distances (Å) bond angles (°): (Pd1-N2 2.124(3), Pd1-N1 2.141(3), Pd1-S1 2.2442(9), Pd1-S2 2.2544(9), N2-Pd1-N1 77.97(13), N2-Pd1-S1 169.96(9), N1-Pd1-S1 96.53(10), N2-Pd1-S2 96.10(10), N1-Pd1-S2 165.06(10), S1-Pd1-S2 91.19(3)).

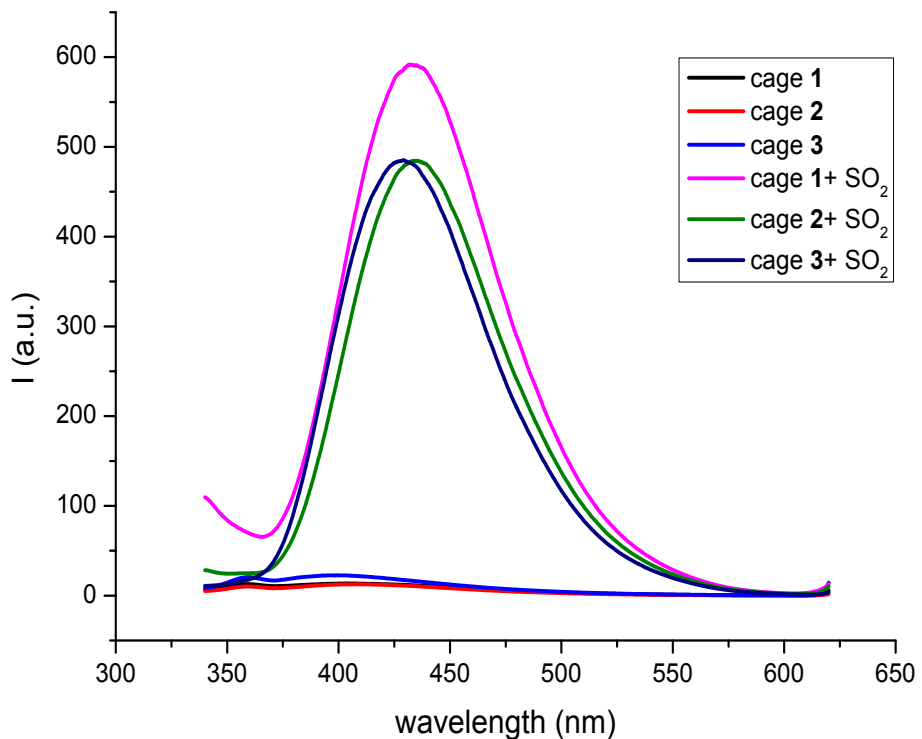


Fig. S27 Changes in fluorescent intensity for cage **1**, cage **2**, cage **3** (1.0×10^{-5} M) in $\text{CH}_3\text{CN}/\text{H}_2\text{O}$ (1:2, v/v) after addition of SO_2 gas.

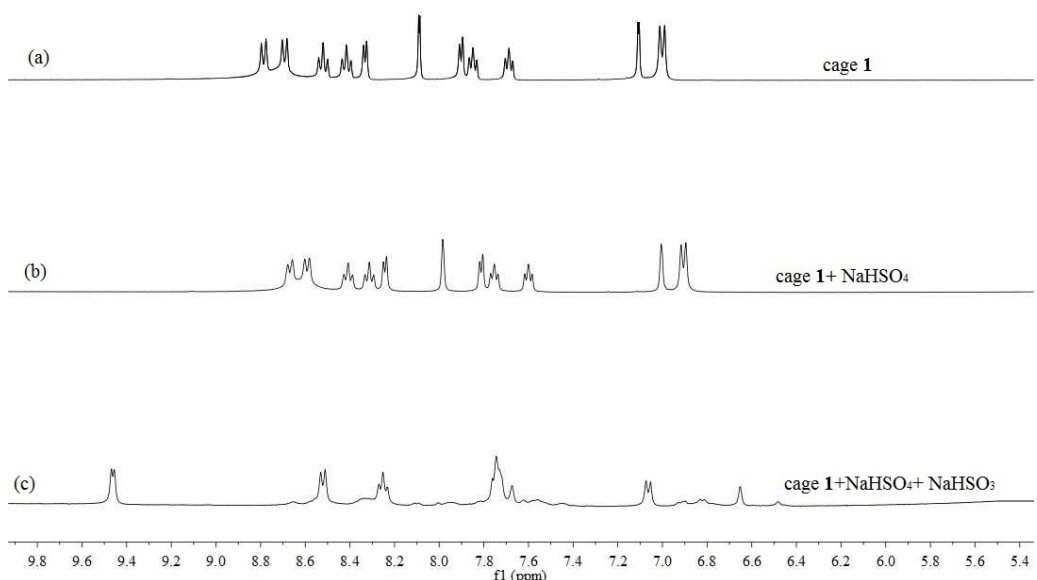


Fig. S28 ^1H NMR spectra of cage **1** (a), cage **1** + NaHSO_4 (b) and cage **1** + NaHSO_4 + NaHSO_3 (c) in $\text{DMSO-d}_6/\text{D}_2\text{O}$ (1:2, v/v).

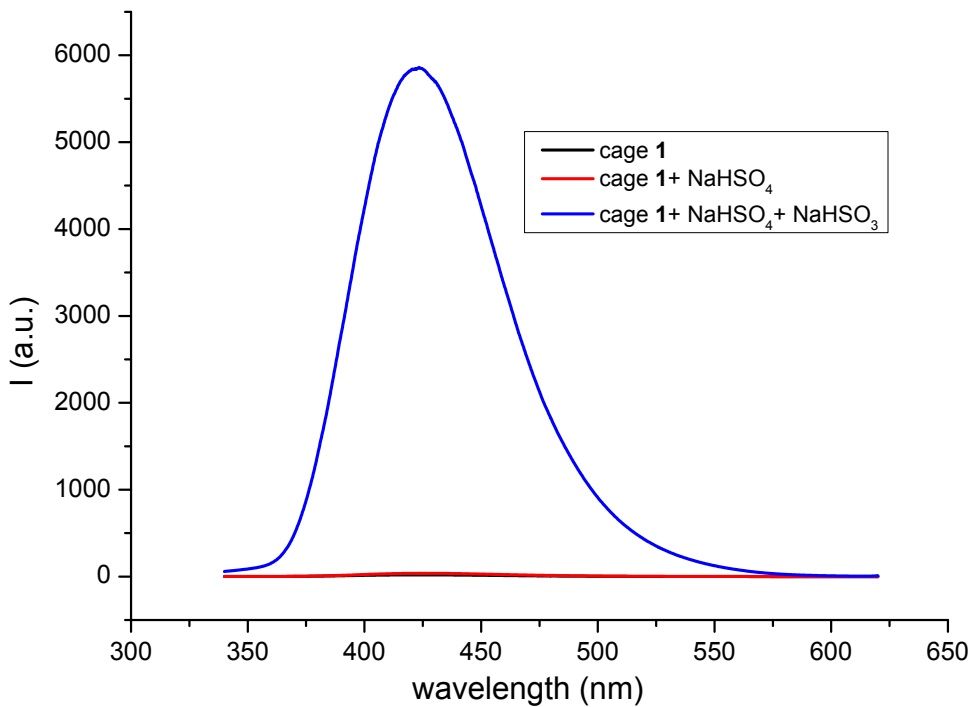


Fig. S29 Changes in fluorescent intensity for cage **1** (1.0×10^{-5} M) in $\text{CH}_3\text{CN}/\text{H}_2\text{O}$ (1:2, v/v) after addition of NaHSO_4 and mixture of NaHSO_4 and NaHSO_3 salt.

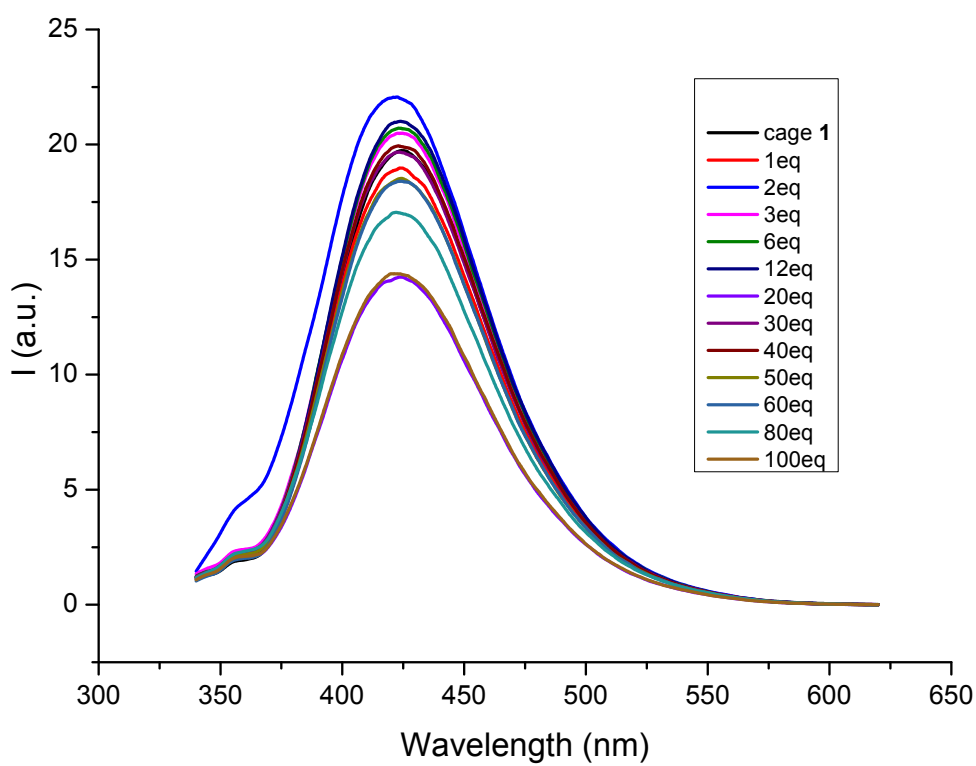


Fig. S30 Changes in fluorescent intensity for cage **1** (1.0×10^{-5} M) in $\text{CH}_3\text{CN}/\text{H}_2\text{O}$ (1:2, v/v) after addition of various equivalents of HSO_4^- .

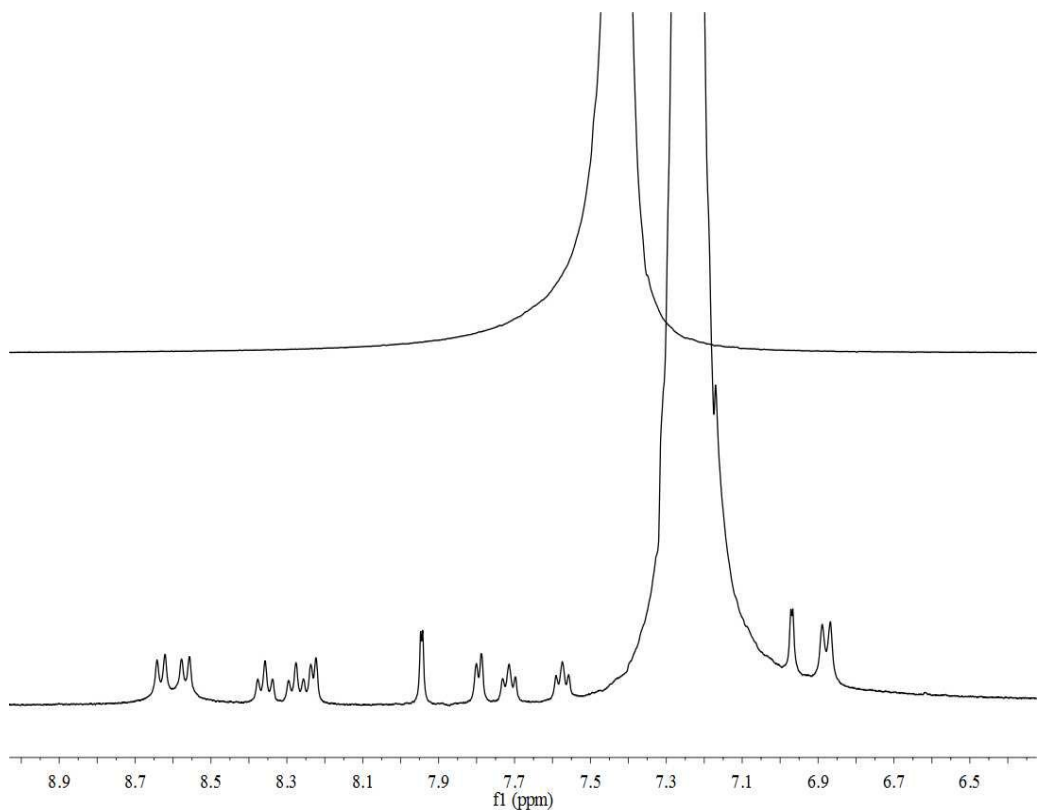


Fig. S31 ^1H NMR spectra of concentrated HNO_3 (top) and cage **1** + concentrated HNO_3 (down) in $\text{DMSO-d}_6/\text{D}_2\text{O}$ (1:2, v/v).

1. W. L. F. Armarego and D. D. Perrin, *Purification of Laboratory Chemicals*, Butterworth Heinemann, Oxford, U. K., 4th edn, 1997.
2. S.-Y. Yu, M. Fujita and K. Yamaguchi, *J. Chem. Soc., Dalton Trans.*, 2001, 3145.
3. Sheldrick, G. M. SHELXS-97 (Univ. Göttingen, 1990).
4. Sheldrick, G. M. SHELXL-97 (Univ. Göttingen, 1997).